Thesis for The Degree of Licentiate of Engineering

N,N-Dialkylamide-Based Solvent Systems for Actinide Separation: A Replacement Strategy for TBP in the CHALMEX Process

Esraa Darwish

Department of Chemistry and Chemical Engineering

Chalmers University of Technology | University of Gothenburg
Gothenburg, Sweden, 2026

N,N- Dialkylamide -Based Solvent Systems for Actinide Separation:

A Replacement Strategy for TBP in the CHALMEX Process

Esraa Darwish

Licentiatuppsatser vid Institutionen för kemi och kemiteknik
Chalmers tekniska högskola.
Technical report Nr. 2026:04

Nuclear Chemistry and Industrial Material Recycling
Department of Energy and Material

Chalmers University of Technology | University of Gothenburg SE-412 96 Göteborg, Sweden
Phone: +46(0)31 772 1000

Cover:

Schematic Illustration of Actinide Extraction Using the $CyMe_4$-BTBP–DBOA Solvent System

Printed by Chalmers Digitaltryck, Gothenburg, Sweden 2026.

_N,N_-Dialkylamide-Based Solvent Systems for Actinide Separation: A Replacement Strategy for TBP in the CHALMEX Process

Esraa Darwish
Nuclear Chemistry
Department of Chemistry and Chemical Engineering
Chalmers University of Technology

Abstract

In Sweden, rising electricity demand has renewed interest in nuclear expansion, and the government is reviewing options to increase capacity. However, expanding nuclear power also increases the need for improved management of spent nuclear fuel.

Used nuclear fuel contains long-lived radionuclides, including Pu and minor actinides (Np, Am, Cm). These nuclides mainly contribute to long-term radiotoxicity and decay heat. Advanced recycling strategies are needed within a closed nuclear fuel cycle. In these, recovered actinides can be integrated into fuels for Generation IV fast reactors. This improves resource use and reduces the long-term burden of the final waste.

A range of recycling processes is under development, including the Grouped Actinide EXtraction (GANEX) process. The Chalmers variation, CHALMEX, is a solvent extraction process. It is designed to recover all actinides together as a group, using a single solvent that combines an O-donor extractant with the N-donor ligand $CyMe_4$-BTBP in the fluorinated diluent FS-13. This enables extraction across relevant actinide oxidation states in a compact flowsheet with a limited number of stages.

In the CHALMEX solvent, tri-n-butyl phosphate (TBP) is used as the O-donor extractant. Its degradation products, formed under acidic and radiolytic conditions, complicate solvent management and impair extraction performance. This work evaluates a phosphorus-free replacement, in which TBP is replaced by the monoamide N,N-dibutyl octanamide (DBOA), with degradation products expected to be more manageable during process operation.

Extractant performance was investigated using a simulated PUREX raffinate containing fission and corrosion products in the presence of masking agents. Solvent stability was assessed by hydrolytic ageing and γ-irradiation up to 300 kGy. The results show that TBP can be replaced by DBOA without compromising key CHALMEX separation functions, while providing better radiolytic stability. In addition to higher Pu extraction with the DBOA-based solvent, this is a potential advantage for Pu-rich feed streams, such as those expected in a GANEX raffinate.

Finally, batch flowsheet tests (extraction–scrub–strip) supported optimization of the CHALMEX system for scale-up and showed that stripping from the DBOA-based solvent is feasible. Building on these findings, further work is needed to link the recycling step to fuel fabrication and to better quantify kinetics under realistic contacting conditions to support scale-up.

KEYWORD: CHALMEX process, N, N-dibutyl octanamide, DBOA, Spent nuclear fuel recycling, Solvent extraction, Actinide separation.

List of Publications

Appended publications

This thesis is based on the following publications:

I. Darwish, E., Hedberg, M., Forman, M., & Ekberg, C.: Investigation of Dialkylamides (DBOA) as a Potential Extractant Agent for Uranium and Plutonium in the CHALMEX Proces**s**. (2026). *Solvent Extraction and Ion Exchange.*
https://doi.org/10.1080/07366299.2026.2624109
Contribution: Main author of the paper and did all the experimental work.

II. Darwish E., Hedberg M., Ekberg C.: Batch Flowsheet Study of the CHALMEX Process: Comparing TBP and Monoamide Extractants.
Manuscript planned for submission to the *Journal of Radioanalytical and Nuclear Chemistry*.
Contribution: Main author of the paper and did all the experimental work.

Abbreviations

The following abbreviations and definitions are used throughout this thesis.

Abbreviation	Definition
An/Ln	Actinide/lanthanide
BTBP	Bis(1,2,4-triazinyl)bipyridine (ligand family)
BTP	Bis(1,2,4-triazinyl)pyridine
CEA	French Alternative Energies and Atomic Energy Commission (Commissariat à l'énergie atomique et aux énergies alternatives)
CHALMEX	Chalmers Grouped Actinide Extraction (process concept)
CHON	Carbon, hydrogen, oxygen and nitrogen only (principle for fully incinerable solvents)
CLAB	Central Interim Storage Facility for Spent Nuclear Fuel (Sweden)
CyMe4-BTBP	6,6′-bis(5,5,8,8-tetramethyl-5,6,7,8-tetrahydrobenzo[1,2,4]triazin-3-yl)[2,2′]bipyridine
DBOA	N,N-dibutyl octanamide
DBP	Dibutyl phosphate
DEHBA	N,N-di(2-ethylhexyl) butyramide
DEHiBA	N,N-di(2-ethylhexyl) isobutyramide
DIAMEX	DIAMide EXtraction (co-extraction of An(III)/Ln(III))
DMDOHEMA	N,N'-(dimethyl)-N,N'-dioctylhexylethoxy malonamide
EURO-GANEX	European Grouped ActiNide EXtraction
FS-13	Phenyl trifluoromethyl sulfone
FTIR	Fourier-transform infrared spectroscopy
GANEX	Grouped ActiNide Extraction
GC-MS	Gas chromatography–mass spectrometry
HDEHP	Di(2-ethylhexyl) phosphoric acid
HEDTA	N-(2-hydroxyethyl)ethylenediamine-N,N',N'-triacetic acid
HNO_2	Nitrous acid
HPGe	High-purity germanium (gamma-ray detector)
IAEA	International Atomic Energy Agency
ICP-MS	Inductively coupled plasma mass spectrometry
ICP-OES	Inductively coupled plasma optical emission spectroscopy
KBS-3	Swedish KBS-3 concept for geological disposal of spent nuclear fuel
kGy	Kilo gray
LWR	Light-water reactor
MA	Minor actinides
MBP	Monobutyl phosphate
MOX	Mixed oxide (fuel)
MWe	Megawatt electric
O/A	Organic-to-aqueous phase ratio
PGM	Platinum group metals
PUREX	Plutonium Uranium Reduction EXtraction
SANEX	Selective ActiNide Extraction
SKB	Svensk Kärnbränslehantering AB
SMR	Small modular reactor
SNF	Spent nuclear fuel
SX	Solvent extraction
TBP	Tri-n-butyl phosphate

TODGA	N,N,N',N'-tetraoctyl diglycolamide
TRU	Transuranic elements
UO_X	Uranium oxide fuel
UV-Vis	Ultraviolet–visible spectroscopy

Contents

1. Introduction

Global electricity demand continues to rise with an estimated annual increase of roughly 2.4%.[1] Nuclear energy, as a low carbon dioxide emission energy source, offers a sustainable solution to meet this growing demand. It provides substantial, dependable electricity, unaffected by weather conditions or seasonal variability. Beyond everyday electricity needs, homes, industry, and electric transport, recent assessments show that rapid AI growth is increasing data-center electricity demand. The International Atomic Energy Agency (IAEA) Bulletin notes this near-continuous load is driving interest in advanced nuclear technologies and small modular reactors (SMRs) for reliable continuously operating, low carbon power.[2]

In Sweden, nuclear energy has long been a key component of the electricity system, accounting for about 30% of total electricity production in 2024.[3]

Sweden's current energy policy positions new nuclear construction as a key element of a longer-term pathway to maintain a fossil-free electricity system while meeting increasing electricity demand. Government communications indicate an ambition to have new nuclear capacity corresponding to at least 2500 MW_e (≈ two large-scale reactors' worth) by 2035 at the latest, followed by a substantially broader expansion toward 2045, potentially on the order of 10 000 MW_e , delivered through a combination of reactor technologies that may include SMRs.[4]

However, the management of spent nuclear fuel (SNF) remains a major challenge.[5] From a sustainability perspective, SNF retains more than 90% of its potential energy. Advanced closed fuel cycle strategies therefore aim to recover fissile and fertile actinides for reuse, while minimizing the long-term radiotoxicity and heat load of the remaining waste.[6,7,8,9]

A fully closed nuclear fuel cycle is mainly about recycling actinides beyond just uranium and plutonium. This includes the possible recycling of minor actinides such as neptunium, americium and curium, with the aim of bringing these nuclides back into the fuel cycle through suitable fuel fabrication routes. To make these concepts practical, fast neutron reactor systems are essential, often discussed in the context of Generation IV systems.[10,11]

In this context, solvent-extraction-based recycling routes play a central role in enabling closed fuel cycle management. Solvent extraction (liquid–liquid extraction) is a separation technique in which solutes distribute between two immiscible liquid phases. Selective transfer is driven by an extractant dissolved in one phase, which forms extractable complexes with target solutes and thereby shifts their distribution between the phases. A well-established example is the PUREX (Plutonium Uranium Reduction Extraction) process, which has been operated industrially in France since the mid-1960s. Among advanced recycling schemes, the Chalmers Grouped Actinide Extraction (CHALMEX) process is designed to recover uranium, plutonium, neptunium, americium, and curium as a single group by combining two extractants tailored to the relevant actinide oxidation states. This supports the recovery and reuse of valuable actinides while remaining proliferation resistant by avoiding single-element product streams.

In previous CHALMEX-oriented studies, tributyl phosphate (TBP)-based solvent systems were widely investigated as traditional extractants. [12, 13, 14, 15] However, TBP has well-known limitations under process-relevant conditions, particularly under irradiation, where radiolytic degradation products can accumulate and adversely affect extraction performance, phase behavior, and operational robustness. [16,17,18,19]

To address these limitations, the present work investigates a phosphorus-free extractant as a potential replacement for TBP within the CHALMEX concept. The monoamide system is evaluated under conditions representative of an industrial recycling environment, including irradiated solvent and realistic raffinate matrices containing fission and corrosion products, and is assessed throughout relevant stages of the flowsheet to establish a comprehensive understanding of its behavior compared with TBP. A key objective is to demonstrate that, under irradiation, the monoamide generates radiolysis products that are expected to be less detrimental to extraction and phase stability, thereby minimizing adverse effects such as third-phase formation and preserving reliable actinide recovery across the process.

2. Background

2.1 Spent nuclear fuel

Nuclear power plants are based on neutron-induced fission of heavy nuclei. In today's light-water reactors, the fuel is typically UO_2 enriched in ^{235}U, and the heat produced comes mainly from fission of ^{235}U, and later in the irradiation, also from fissile plutonium isotopes that form in the fuel.[20] During operation, the fuel is exposed to an intense neutron flux. Besides fission, neutron capture takes place, especially in ^{238}U, and a sequence of neutron capture and β-decay reactions gradually builds transuranium elements (Np, Pu, Am, Cm) inside the fuel matrix.[21]

The fuel is discharged from a reactor once it reaches the licensed burnup limit, typically when the reactivity of the fuel has decreased due to the buildup of neutron-absorbing fission products (fission-product poisoning).[22] The residence time of fuel in the core varies based on reactor type, fuel design and burnup targets but is commonly on the order of three to five years.[23] Once discharged the material is considered spent, or used, nuclear fuel. It is still highly radioactive and releasing decay heat, so cooling and shielding are still necessary prior to any further handling.[24]

In practice, spent nuclear fuel has a highly complex composition, containing a wide range of elements. The exact composition depends on factors such as initial enrichment, burnup, reactor type, power history, and cooling time.[8, 25] Even so, representative values–are useful for clarifying the scale of the separation challenge. For example a typical light water reactor (LWR) UO_X fuel after 50 GWd/tHM (gigawatt-days of thermal energy per ton of heavy metal), the spent fuel composition can be summarized (mass %) as: U 93.4%, 1.2% Pu, 0.2% minor actinides (Np, Am, Cm), 5.2% fission products.[26] On the fission product side, the mixture is chemically diverse and spans much of the periodic table, in total, more than 400 distinct fission fragments can be formed. Moreover, in dissolved spent nuclear fuel, the lighter actinides may exist in multiple oxidation states, which governs their aqueous speciation.

2.2 Strategies for Spent Nuclear Fuel Management

Nuclear power produces a relatively small volume of waste per unit of electricity, but some radioactive materials still require long-term management. Nuclear waste is typically classified as low, intermediate, and high-level. [27] Most of the volume is low-level operational waste with limited radioactivity. Whereas high-level waste, primarily used (spent) nuclear fuel, accounts for a small fraction of the volume (3% of the total volume) but contains most of the radioactivity. In many regulatory frameworks, waste is also distinguished by its longevity, short lived, intermediate, and long-lived, because this affects the required containment period and disposal concept.[28]

Countries take different paths for managing highly radioactive waste once it leaves the reactor. In many cases, the main long-term solution is deep geological disposal. So far, Sweden and Finland are the countries that have most clearly advanced their own deep geological repository programs.

In Sweden, Svensk Kärnbränslehantering AB (SKB) is developing a repository system following the well-known KBS-3 concept, a multi-barrier approach based on a corrosion-resistant copper canister, a bentonite clay buffer, and the long-term stability of the Swedish crystalline bedrock.[29,30]

While other countries follow different approaches, developing disposal options more slowly, relying on interim storage, and, in some cases, choosing to reprocess and recycle spent fuel to varying degrees, in addition to planning for final disposal.

Advanced reprocessing increasingly favors extractants that follow the CHON principle (C, H, O, and N only).[31] This enables complete incineration of the organic phase and can reduce secondary waste generation after separation. Since the 1990s, CHON compliance has therefore been widely discussed as a key criterion when selecting extractants for recycling-oriented flowsheets.[32] Nevertheless, even with a fully closed nuclear fuel cycle and the widespread deployment of Generation IV systems, that could significantly reduce the required isolation time, a geological repository remains necessary for the ultimate disposal of residual wastes.

2.2.1 Open fuel cycle (once-through)

Sweden uses an open (once-through) fuel cycle in which spent nuclear fuel is first cooled in interim storage before being prepared for final disposal. The interim storage facility is CLAB (Central Interim Storage Facility for Spent Nuclear Fuel) which currently stores about 8,000 tons of spent fuel, with a total capacity of around 11,000 tons.[33]

Here, the fuel cycle concludes with interim storage followed by geological disposal. The advantage is that the once through system avoids chemical separation operations and other manipulation of the intact fuel bundles. However, it also means that uranium, plutonium, and minor actinides remain in the final waste and thus the long-term radiotoxicity is strongly governed by the actinide inventory. As a result, the spent fuel may require more than 100,000 years for its radiotoxicity to decrease to the level of natural uranium ore (see Figure 1).[34, 35]

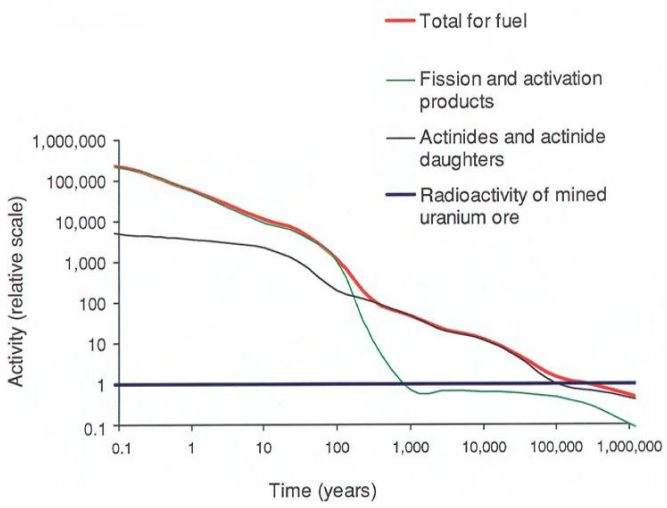

Figure 1. Relative activity of spent nuclear fuel of type SVEA 64 with a burnup of 38 GWd/t U. The activity is dominated during the first 100 years by fission products, thereafter by actinides.[36]

2.2.2 Closed fuel cycle

The second option for managing spent nuclear fuel is a closed or semi-closed fuel cycle. Within this recycling framework, several strategies can be considered, ranging from single plutonium recycling to fabricate mixed oxide fuel (MOX), to more advanced approaches that aim to recycle plutonium and minor actinides for use in Generation IV fast reactors, as shown in Figure 2.

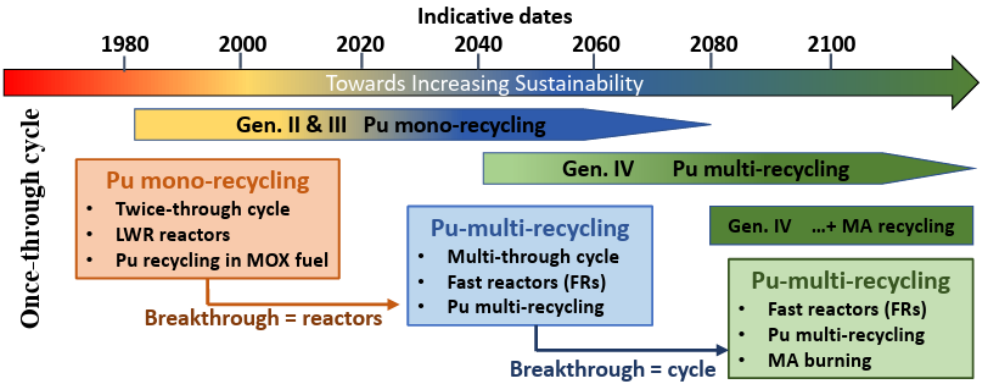

Figure 2. Roadmap of Fuel-Cycle Generations: Transition from Once-Through to Pu/MA Multi-Recycling.[8]

The common link between these recycling variants is their impact on the long-term radiotoxicity of the final waste stream sent for geological disposal. By moving from no recycling to Pu-only recycling, and finally towards recycling (and transmuting) Pu and minor actinides, the residual waste becomes progressively less dominated by long-lived actinides. This shifts the "radiotoxicity tail" to much shorter timescales (Figure 3).[7]

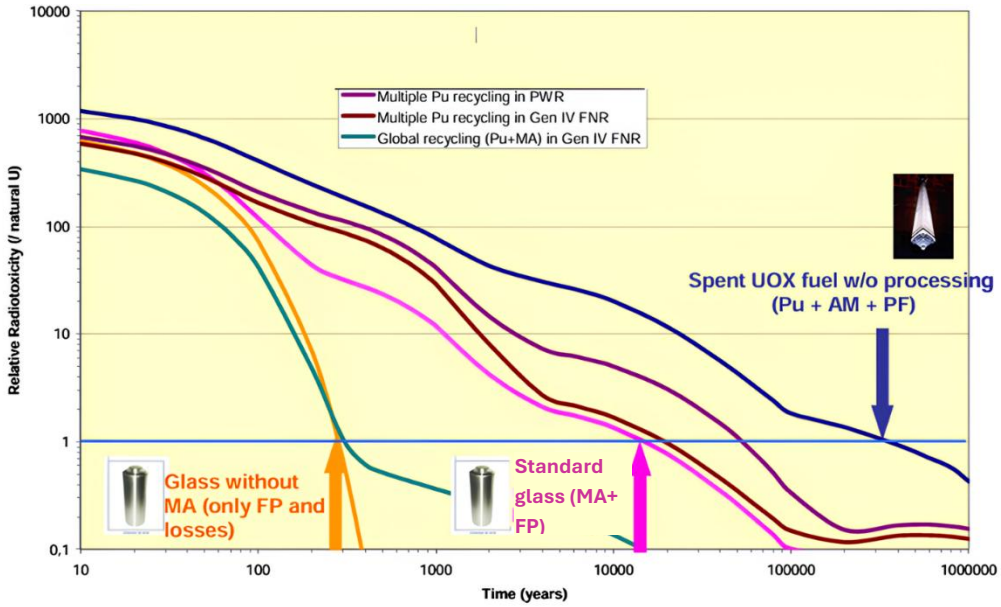

Figure 3. Impact of Actinide Recycling Strategy on the Long-Term Radiotoxicity of Nuclear Waste.[7]

Broadly, reprocessing options are often grouped into dry and wet routes. Dry routes (pyroprocessing) rely on high-temperature chemistry. These methods can offer advantages such as improved radiation tolerance and, in some designs, reduced criticality concerns, but they are generally less established for large-scale deployment. In contrast, the wet route, based on hydrometallurgical approaches, typically begins with dissolution of the fuel in nitric acid, followed by solvent extraction.

Recycling strategies are also commonly described as either homogeneous or heterogeneous: in homogeneous recycling, minor actinides are recycled together with plutonium in a single fuel matrix, whereas in heterogeneous recycling they are separated into individual, high-purity streams.[37]

2.2.2.1 PUREX process

The PUREX process is the established industrial standard, where uranium and plutonium are extracted from nitric acid solutions using TBP in a hydrocarbon diluent, producing separate uranium and plutonium product streams and leaving most fission products and minor actinides in the aqueous raffinate. [38,39]

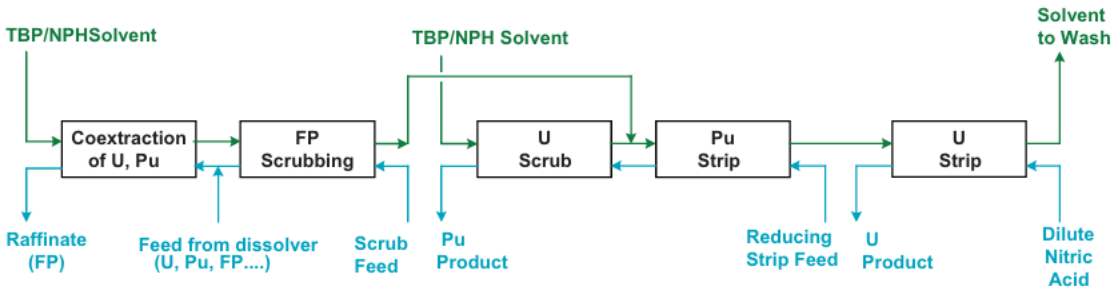

Figure 4. Flowsheet diagram for PUREX process.[40]

PUREX has two well-known limitations in the context of more advanced fuel cycles. First, it does not recover the minor actinides, they remain in the high-level waste stream. Second, it produces separated actinide product streams (especially plutonium) that raise proliferation-sensitivity concerns and motivate alternative approaches. [41]

To enable recovery of minor actinides from the PUREX process, a range of advanced aqueous (post-PUREX) partitioning steps has been developed to treat the high-active raffinate. In the French/European strategy, DIAMEX (DIAMide EXtraction) employs malonamide-type extractants to co-extract trivalent minor actinides together with the lanthanides from the PUREX raffinate, while the majority of other fission products remain in the aqueous phase. The combined An(III)/Ln(III) product stream from DIAMEX is subsequently treated by

SANEX (Selective ActiNide EXtraction), which uses actinide-selective chemistry to separate Am/Cm from the lanthanides. This yields an actinide-rich stream suitable for recycle target fabrication, and lanthanide-rich stream that goes to final waste processing.[42]

2.2.2.2 GANEX process (Grouped ActiNide EXtraction)

A step toward Generation IV spent-fuel reprocessing, advanced solvent extraction processes such as GANEX and derived flowsheets have been developed. The process was initially developed by the French Alternative Energies and Atomic Energy Commission (CEA) as a two-cycle solvent extraction scheme.

The GANEX process is a homogeneous recycling concept in which the aim is to keep transuranic elements together (Np, Pu, Am, Cm), rather than producing separate purified streams. This approach can improve proliferation resistance while still supporting advanced fuel fabrication strategies. The process is typically described as a two-cycle scheme:

1. The first cycle of GANEX is designed to selectively remove the bulk uranium fraction from dissolved spent nuclear fuel using the branched monoamide extractant DEHiBA [*N,N*-di(2-ethylhexyl) isobutyramide], which offers high uranium loading capacity and good selectivity against Pu(IV) and other actinides. This step reduces solvent loading and makes later fuel-fabrication adjustment easier, since uranium is present in much larger quantities than other actinides
2. The second cycle, the transuranic (TRU) elements are separated from the remaining fission products. In this approach the actinides and lanthanides will be co-extracted and then separated through selective back-extract steps using an aqueous complexation agent/stripping agent that binds actinides more strongly, or differently than lanthanides. Such as water-soluble BTP. [43]

The CEA-GANEX flowsheet consist of a malonamide DMDOHEMA [N,N'-(dimethyl)-N,N'-dioctylhexylethoxy malonamide] and HDEHP [di-2-ethylhexyl phosphoric acid] used together to co-extract actinides and lanthanides. Then an actinide-selective stripping step is often done with HEDTA and citric acid (pH ~3).[44]

An alternative to the CEA-GANEX scheme was explored, leading to the development and testing of the EURO-GANEX cycle. Where EURO-GANEX flowsheet replaces the HDEHP solvent with a [Diglycolamides N,N,N′,N′-tetraoctyl diglycolamide] TODGA-based solvent: TODGA and DMDOHEMA in a hydrocarbon diluent (often Exxsol D80 / kerosene).[45, 46]

In more recent schemes, the stripping chemistry can be further tuned to separate Am from Cm, enabling targeted americium recovery while curium is retained or recovered under different conditions.

2.2.2.3 CHALMEX process

The CHALMEX (Chalmers GANEX) concept aims to co-extract all actinides without redox control in a single solvent system, thereby simplifying flowsheets compared with processes that use separate cycles for U/Pu and minor actinides.

The main distinction between CHALMEX and many GANEX variants is where selectivity is introduced. In CHALMEX, the separation relies primarily on selective extraction, achieved by including actinide-selective organic ligands so that actinides are preferentially transferred to the organic phase, while lanthanides remain mainly in the aqueous phase.

3. Theory

3.1 Chemistry of Actinides (f – elements)

The unique electronic structure of the actinides, most notably the energetic similarity between the 5f, 6d, and 7s valence orbitals, allows for a wide range of accessible oxidation states among the lighter actinides. Theoretically from +I to +VII. [47,48,49] In practice the stability of each oxidation state is highly dependent on factors such as the redox environment, ligand identity, and acidity of the solution.[50,51,52]

The most stable states of actinides in nitric-acid media (similar to those in spent nuclear fuel) are shown in Table 1. Notably, early actinides can adopt unusually high oxidation states and tend to form covalent bonds with oxygen (so called -yl ions). [53] These species are typically linear with the structure O=An=O (AnO_2^+, AnO_2^{2+}), characterized by strong axial An=O bonds. Ligand binding in these species is largely restricted to the equatorial plane.[53] Uranium is commonly found in the uranyl ion UO_2^{2+}, while neptunium commonly exists as (NpO_2^+). [47]

This redox speciation significantly influences structural characteristics. Non-actinyl actinides (trivalent and tetravalent) generally exhibit high coordination numbers and flexible geometries. with coordination spheres dominated by water and nitrate ligands.

Table 1. Most Common Oxidation States and Electron Configurations of Actinides Relevant to Spent Fuel Recycling. [47]

Element	Most common ox. state ***(most stable in bold)***	Electron configuration in the ground state
U	+III; +IV; +V; **+VI**	[Rn]$5f^3$ $6d^1$ $7s^2$
Np	+III; +IV**; +V**; +VI; +VII	[Rn]$5f^4$ $6d^1$ $7s^2$
Pu	+III; **+IV**; +V; +VI	[Rn]$5f^6$ $7s^2$
Am	**+III**; +IV; +V; +VI	[Rn]$5f^7$ $7s^2$
Cm	**+III**; +IV	[Rn]$5f^7$ $6d^1$ $7s^2$

Across the actinide series, a gradual decrease in ionic radii occurs,(Figure 5) [54] known as the actinide contraction. This phenomenon results from the poor shielding effectiveness of the 5f electrons, which allows the increasing nuclear charge to draw valence electron density progressively closer to the nucleus from Th to Lr.[54] A similar trend is observed in the lanthanide series, though there are important distinctions. In lanthanides, the 4f orbitals are more effectively shielded by the 5s and 5p electrons, leading to weaker orbital participation in

bonding. As a result, lanthanide chemistry is predominantly governed by ionic size and charge, rather than covalency.[55]

The size difference between trivalent lanthanides and trivalent actinides is relatively small, leading to chemical similarities between ions like Am(III) and Cm(III) and their lanthanide counterparts. This overlap in chemical behavior presents a major challenge for achieving effective intergroup separation during advanced reprocessing.[56] Nevertheless, such separations are critical for reprocessing applications, as some lanthanides, such as samarium, europium, and gadolinium have high neutron-absorption cross sections that negatively affect reactor performance. Separating Am(III) from Cm(III), however, remains one of the most technically difficult steps due to their nearly identical chemical properties.

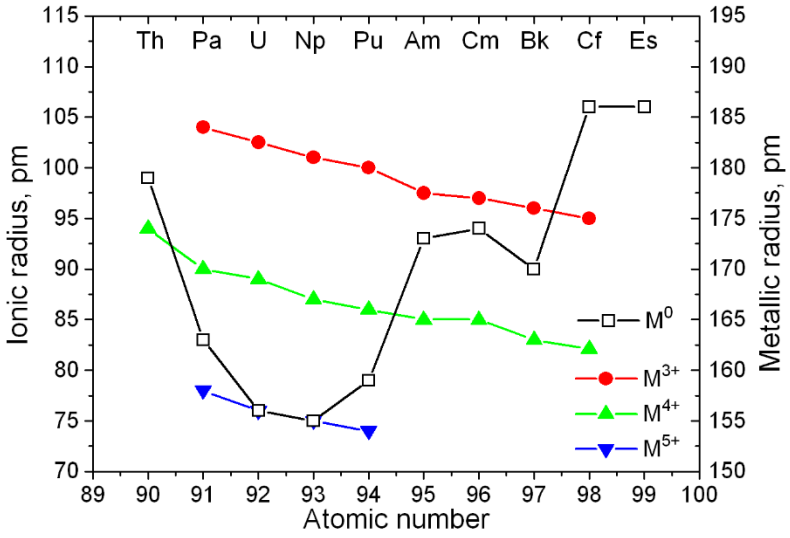

Figure 5. Ionic radii of selected actinide oxidation states as a function of atomic number. [54]

3.2 Solvent extraction

Also called Liquid–liquid distribution in IUPAC terminology (sometimes also called liquid–liquid extraction),[57] commonly referred to SX in hydrometallurgy and nuclear fuel reprocessing. The principle of this separation method is based on the distribution of solutes between two immiscible liquid phases. Typically, these phases are an aqueous electrolyte phase and an organic phase in contact with each other. The distribution is driven by differences in solvation and chemical interactions of the solute in the two media. [58]

Solvent extraction may be nonreactive (simple distribution of a single solute species by solubility) or reactive, where chemical reactions form extractable complexes/adducts with an extractant; most practical metal-ion extraction processes (hydrometallurgy and reprocessing) rely on such reaction-based mechanisms.[59]

The overall extraction rate may be controlled either by mass transfer (diffusion through boundary films) or by interfacial chemical reaction kinetics. If the process is diffusion-controlled, increasing the surface area between the phases increases the extraction rate. In

contrast, if the process is controlled by interfacial reaction kinetics, the extraction rate shows little or no dependence on interfacial area once adequate mixing is achieved.[60,61,62]
Solvent extraction is widely used for recycling and purification, especially in metallurgical and mining operations. It is also applied across diverse industries, from producing high-purity pharmaceuticals and biomedical compounds to separating heavy organics and metals, and it remains important in analytical chemistry and environmental waste treatment.[63,64]

A typical SX system consists of:

- Extractant(s): ligands that bind the target species, responsible for the complexation.
- Diluent: bulk organic medium controlling polarity, viscosity, density, flash point, etc.
- Optional modifiers/stabilizers: prevent third phase formation, adjust phase behavior, or improve stability.

3.2.1 Extraction mechanisms

Two common extraction mechanisms are discussed:

1. Solvation (neutral) extraction

Where a solvating extractant transfers a metal to the organic phase by replacing coordinated water molecules and solvating a neutral metal complex. A classic example for solvating extractants is TBP. A general solvation equilibrium can be written as:

$$M_{(aq)}^{z+} + zX_{(aq)}^{-} + mL_{(org)} \rightleftharpoons M(X)_z.mL_{(org)} \qquad (1)$$

Where: M the metal , L the ligand. X anion in the aqueous phase

Neutral complexes between a metal ion and a ligand. The complexes are, however, coordinatively unsaturated and can therefore accept uncharged organic molecules as solvating agents. This class is therefore often called solvating extraction. [58]

2.Ion pair extraction
This can proceed by either:
a) Anion-pair extraction (most common) is formed between an anionic metal complex and one or more large organic cations.

$$ML_n^{X-} + xQL_{(org)} \rightleftharpoons Q_xML_{n_{(org)}} + xL^{-} \qquad (2)$$

b) Cation exchange mechanism like Acidic extractants.
An acidic extractant transfers a metal into the organic phase via cation exchange, where the metal binds to the deprotonated extractant and an equivalent number of protons are released to the aqueous phase. This mechanism is common in hydrometallurgy and is useful mainly as a contrast when interpreting pH-dependent extraction behavior.

$$M_{(aq)}^{n+} + nHA_{(org)} \rightleftharpoons MA_{n_{org}} + nH_{(aq)}^{+} \qquad (3)$$

Where: M denotes the metal and HA the undissociated extractant. [58]

3.2.2 Quantification of extraction performance

The distribution ratio, D_M, is defined as the ratio of total analytical concentration of a solute (M) in the organic phase to that in the aqueous phase at equilibrium. It quantifies the extent to which solute is extracted into the organic phase under the given conditions.

$$D_M = \frac{[M]_{org}}{[M]_{aq}} \qquad (4)$$

Selectivity between two solutes (e.g., An /Ln) is quantified by the separation factor, with the convention $SF > 1$.

$$SF_{A/B} = \frac{D_A}{D_B} \qquad (5)$$

Stripping is quantified as stripping efficiency, defined as the percentage of the metal inventory in the loaded organic phase transferred to the stripping aqueous phase in a single contact. In case of volume ratio of the phases (θ =1) stripping efficiency is calculated as eq 6.

$$E_{\%} = 100 \times \left(\frac{1}{1+ D_{strip}}\right) = \left(100 \times \frac{[M]_{aq}}{[M]_{org} + [M]_{aq}}\right) \qquad (6)$$

Where $[M]_{org}$ and $[M]_{aq}$ are the concentrations of a metal ion in the loaded organic phase before stripping and in aqueous phase after stripping, respectively.

3.3 Design of SX Flowsheets

An industrial solvent-extraction flowsheet typically comprises two essential operations: extraction, and stripping, as shown in (Figure 6) Depending on the required product purity and the selectivity of the extraction step, an intermediate scrubbing stage may be included to further purify the loaded organic phase.

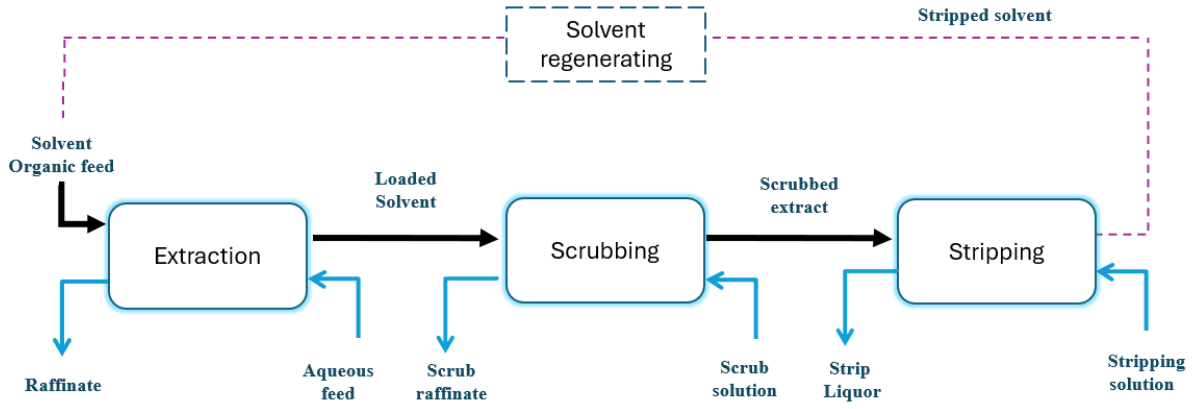

Figure 6. Typical solvent-extraction flowsheet.

At industrial scale, achieving satisfactory extraction and separation is typically not possible in a single stage; therefore, multistage extraction is employed to reduce overall process costs and minimize waste generation. Among the available configurations, counter-current contactors are most commonly used because they maximize mass-transfer efficiency while minimizing solvent consumption. [58]

The regenerated solvent is then recycled to the extraction stage and reused until its performance deteriorates.

3.3.1 Stripping (back-extraction)

Stripping can be achieved through different chemical driving forces:

The first approach is complexation stripping, where an aqueous ligand forms new stable metal complexes, this will pull the extracted metal out of the solvent. Glycolic acid is a good example of a ligand that works well for this purpose.

Glycolic acid is a weak monoprotic acid with a pK_a of around 3.8 at 25 °C. At a slightly acidic pH it becomes largely deprotonated, producing the glycolate ion ($HOCH_2COO^-$). This is the simplest α-hydroxy-carboxylate, can coordinate to metal ions using its carboxylate group (one or both oxygen atoms), and sometimes its α-hydroxyl group as well. The exact coordination depends on the metal ion involved.

The second approach is changing the aqueous anion activity which led to destabilization of the extracted neutral complexes and reducing extraction. Typically, the complexation process provides a stronger thermodynamic drive for stripping than just reducing ions levels.

In addition to these two commonly used approaches, several other stripping strategies are available. Redox stripping involves adjusting the oxidation state of the metal to a form that is less strongly extracted by the organic phase (a classic approach for Pu and Np systems). Precipitation stripping drives transfer by forming an insoluble solid in the aqueous phase.[65] Finally, temperature-swing stripping can be applied when the extraction equilibrium is sufficiently temperature dependent.

3.4 CHALMEX solvent

The Chalmex solvent consists of two extractants with complementary selectivity to cover a broader range of actinide oxidation states

1. Oxygen-donor extractant. Traditionally TBP or DBOA to extract hexavalent uranium and tetravalent plutonium.[66,13,12]
2. Nitrogen-donor extractant, 6,6′-bis(5,5,8,8-tetramethyl-5,6,7,8-tetrahydrobenzo[1,2,4]triazin-3-yl)[2,2′]bipyridine($CyMe_4$-BTBP) is designed to extract primarily trivalent actinides, and separate them from trivalent lanthanides, and also extract pentavalent actinides.

In the CHALMEX systems, phenyl trifluoromethyl sulfone (FS-13) has been used as a polar and relatively dense diluent and has been reported to provide good robustness towards both radiolysis and hydrolysis in nitric-acid environments.[14,67,68] However, one of the drawbacks of the diluent is that FS-13 does not fully comply with the CHON principle.

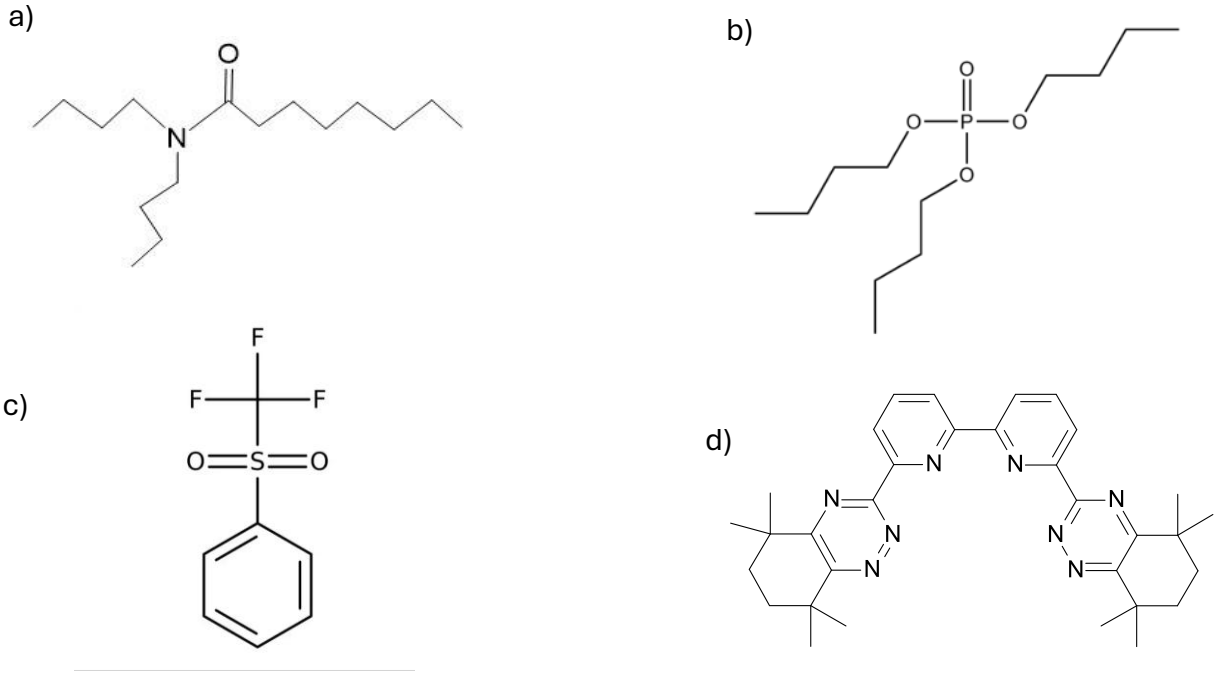

Figure 7. Molecular structure of a) DBOA b) TBP c) FS-13 d) CyMe$_4$-BTBP

The development and evaluation of the CHALMEX solvent follow a structured workflow that assesses actinide extraction performance under representative nitric-acid conditions, optimizes the solvent formulation by examining how extractant concentrations and other parameters influence distribution ratios, selectivity, and phase behavior, investigates fission product behavior with emphasis on co-extraction tendencies and scrub efficiency, evaluates hydrolytic and radiolytic stability to identify degradation pathways and their impact on process performance, and develops and optimizes a batch flowsheet by refining stagewise extraction–scrub–strip conditions to maximize actinide recovery and decontamination.

3.4.1 Monoamide as extractants

A potential replacement for the traditional TBP extractant can be *N,N*-dialkylamides (R–C(O)–NR′$_2$), which follow the CHON principle. Their suitability to replace TBP requires that the aliphatic substituents (R and R′) are appropriately optimized. Where monoamides show synthetic flexibility, as variations in alkyl chain length and branching can be adjusted to design the metal selectivity.[69,70, 71,72]

N,N dialkylamides coordinate with metal nitrates through carbonyl oxygen, where the carbonyl stretching frequency of these amides is significantly lower than that observed for typical carbonyl compounds (Keton), a shift commonly attributed to resonance between the neutral amide form (I) and the charge-separated form (II). Increased contribution from structure (II) not only weakens the C=O bond but also increases the electron density and donor availability at the oxygen atom. thereby promoting coordination and bond formation with metal ions.[73] This electronic feature explains the solvation of metal–nitrate species by N,N-dialkylamides.

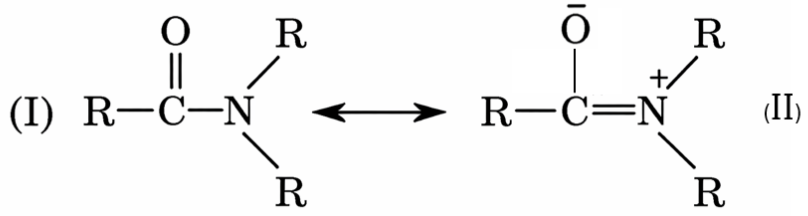

Figure 8. Resonance structures of N,N-dialkylamides (amide functionality).

At low aqueous acidities, dialkylamides act primarily as neutral solvating extractants, coordinating via carbonyl oxygen and forming organic complexes. [73]

$$xM^{n+} + x.nNO_3^- + p\ Amide_{(org)} \rightleftharpoons M_x(NO_3)_{x.n}(Amide)_{p_{(org)}} \quad (7)$$

As the acidity (and nitrate activity) increases, the extraction mechanism shifts and amides can effectively behave as anion-exchange partners. While the amide is largely present as the monosolvate HNO_3.Amide. Actinides are transferred to the organic phase predominantly as nitrato anionic species, such as uranyl nitrato complexes , while the amide becomes protonated and resides in the outer-coordination sphere, forming ion pairs that stabilize these anionic metal–nitrate complexes in the organic phase.[74]

$$UO_2{}^{2+} + 2NO_3^- + HNO_3.Amide + y\ Amide_{(org)} \rightleftharpoons UO_2(NO_3)_3H(Amide)_{y+1_{(org)}} \quad (8)$$

3.5 Radiolytic stability in solvent extraction

3.5.1 Radiolytic environment in HNO_3 systems

Radiolytic stability describes how well a solvent extraction system, consisting of extractant, diluent and any other modifier, can resist chemical and performance changes while exposed to ionizing radiation. In nuclear fuel reprocessing, both the organic and aqueous phases are irradiated by α-, β-, and γ- emitting nuclides present in the dissolved fuel. As a result, radiolysis can alter process chemistry and the physical properties of the phases, and it may even promote third-phase formation. These changes can reduce extraction performance, for example, by lowering the effective extractant concentration or by generating degradation products that interfere with metal complexation.

Radiolysis is the transfer of energy from radiation to matter. When the deposited energy is sufficient to ionize molecules, the extent of energy deposition is commonly expressed as the absorbed dose, which represents the radiation energy absorbed per unit mass of material.

Water radiolysis produces both oxidizing and reducing reactive species, including •OH, e_{aq}^-, and H•. Among these, the most reactive oxidants are •OH and H_2O_2, while the strongest reducing agents are the hydrated electron and the hydrogen atom. Whether the medium behaves overall as oxidizing or reducing depends strongly on the presence of scavengers such as dissolved oxygen and other solutes.[75]

Under typical reprocessing conditions, the aqueous phase contains nitric acid, which efficiently scavenges the hydrated electron and, together with dissolved oxygen, suppresses reducing pathways. This shifts the system toward an overall oxidizing environment, dominated by •OH as well as nitrate/nitrite radical chemistry in HNO_3.

The •OH radical can oxidize organic molecules by electron transfer, abstract hydrogen atoms to form carbon-centered radicals, or add to unsaturated structures. Any of these pathways can initiate degradation chains that may propagate into the organic phase. [76,77,78]

-Nitrate scavenging of electrons

$$NO_3^- + e_{pre}^- \rightarrow NO_3^{2\bullet -} \qquad (9)$$

$$NO_3^- + e_{aq}^- \rightarrow NO_3^{\bullet 2-} \qquad (10)$$

Where e_{pre}^- refers to pre-solvated (prehydrated) electron formed immediately after ionization.

$$NO\bullet_3^{-2} + H_2O \rightarrow NO_2^{\bullet} + 2OH^- \qquad (11)$$

•OH reaction with undissociated nitric acid (NO_3• formation; slow pathway)

$$\bullet OH + HNO_3 \rightarrow H_2O + \bullet NO_3 \qquad (12)$$

In mixed organic systems, the component with the lowest ionization potential often acts as an "ionization sink," absorbing a larger share of the energy and thereby shaping which molecules undergo the most damage. This highlights an important point: the diluent is not merely an inert carrier; its radiolysis products can significantly influence and sometimes dominate extractant degradation. In this context, one key advantage of FS-13 is its relatively high radiolytic stability, which helps limit the formation of aggressive diluent-derived radicals and can improve the robustness of the organic phase under irradiation.

Practically, these effects are often quantified through dose-dependent concentration measurements and dose constants that summarize the rate of chemical change per absorbed dose.

3.5.2 Extractant degradation mechanisms under irradiation

The *N,N*-dialkylamides extractants can gradually degrade under ionizing radiation during spent fuel processing. Radiation produces reactive species in the organic phase either by direct energy deposition in DBOA or indirectly through radical formation in the nitric acid, followed by radical attack on DBOA.

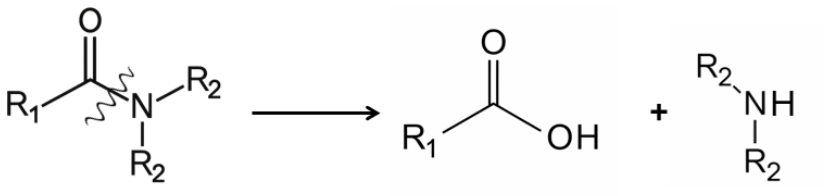

Figure 9. General degradation products of N,N-dialkylamides formed via hydrolytic amide-bond scission during γ-irradiation.

A common degradation pathway is N-dealkylation, where C–N(alkyl) bonds are cleaved to form secondary and/or primary amides and release alkyl amines. In addition, cleavage involving the amide functionality can yield the corresponding carboxylic acid, along with amine-containing fragments.

A simplified hydrolysis reaction for DBOA is:

$$CH_3(CH_2)_6C(=O)N(CH_2CH_2CH_2CH_3)_2+H_2O\longrightarrow CH_3(CH_2)_6COOH+HN(CH_2CH_2CH_2CH_3)_2$$

TBP degrades in nitric-acid media due to the combined effects of acid hydrolysis in HNO_3 and radiation damage (α and γ fields). The dominant pathway is cleavage of the P–O–C (butyl–oxygen) bonds, which produces progressively dealkylated phosphate esters. This yields dibutyl phosphate (DBP/HDBP) and monobutyl phosphate (MBP/H_2MBP) as primary products and, under extensive degradation, ultimately phosphoric acid (H_3PO_4).[18]

Because both DBP and MBP are acidic and strongly coordinating, their accumulation can change phase behavior and metal speciation through the formation of persistent metal–phosphate complexes, thereby reducing extraction and stripping performance. In addition, crud can form from precipitates involving zirconium and TBP degradation products (HDBP and H_2MBP)[79]. MBP is particularly problematic because of its tendency to form precipitate complexes with Pu(IV).[39]

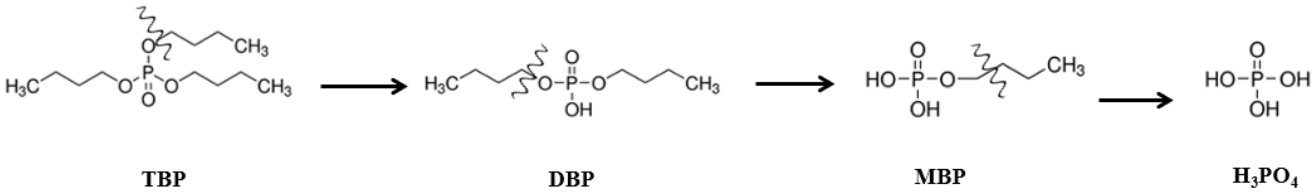

Figure 10. General degradation products for TBP

4. Materials and methods

4.1 Material

The organic phase was formulated using in-house synthesized DBOA , TBP (Sigma-Aldrich), FS-13 purchased from Marshallton Co., Ltd. (China), and $CyMe_4$-BTBP purchased from Technocomm (UK).

The aqueous phases were prepared as nitric acid solutions at concentrations relevant to GANEX-type conditions. 3.0 M HNO_3 was used as the reference acidity.
A synthetic PUREX raffinate was prepared to simulate a CEA-HAW-type PUREX raffinate matrix, containing representative concentrations of corrosion products, lanthanides, and fission products. The composition and concentrations are provided in Appendix 1. All inactive chemicals used to prepare the simulated raffinate solution were analytical grade, commercially available. Actinides and the radioactive lanthanide tracer were introduced at trace levels from stock solutions (^{239}Pu, ^{241}Am, ^{237}Np, ^{244}Cm, ^{152}Eu, and natural uranium). The activities for the stock solutions are provided in Appendix 2.

Organic phase preparation
Unless otherwise stated, two baseline solvent systems were used:

- DBOA system (standard)**:** 30 vol.% DBOA (≈ 1.01 M), 70 vol.% FS-13, and 25 mM $CyMe_4$-BTBP.
- TBP reference system (standard**):** 10 vol.% TBP (≈ 0.37 M), 90 vol.% FS-13, and 25 mM $CyMe_4$-BTBP.

To evaluate formulation effects, the concentrations of DBOA/TBP and $CyMe_4$-BTBP were varied systematically. Organic phases were pre-equilibrated with 3 M HNO_3 prior to experiments to minimize mutual solubility effects and stabilize phase composition.

4.2 Batch solvent extraction experiments

Equal volumes of organic and aqueous phases (400µL each) were contacted in 3.5 mL glass vials. Mixing was performed using a mechanical shaker (IKA Vibrax VXR) at 1500 rpm. Experiments were performed at 298 K using a thermostatic circulating bath. Samples were allowed to settle (~5 min) before phase sampling.

Preliminary kinetics tests confirmed that equilibrium for the investigated actinides was reached within 1 h under the applied conditions. Therefore, a contact times of 60 min (3 M HNO_3) and 75 min (simulated raffinate, including masking agents) were used as standard.

To suppress extraction of problematic fission products, 0.2 M D-mannitol and 20 mM Bimet (The structure is shown in Appendix 3.) were added to the aqueous phase prior to contacting.

4.3 Solvent stability

4.3.1 Hydrolytic stability protocol

Hydrolytic stability was assessed by static aging of the organic phase (25 mM $CyMe_4$-BTBP + 40 vol.% DBOA in 60 vol.% FS-13) in contact with an equal volume of 3 M HNO_3 at room temperature. Prior to aging, the phases were manually mixed to ensure initial equilibration. At predetermined time intervals, organic aliquots were withdrawn and directly evaluated in fresh extraction tests against 3 M HNO_3 containing radionuclide tracers.

4.3.2 Radiolytic stability

The organic solvents were irradiated using a ^{60}Co γ-source (Gamma Cell 220). Irradiations were performed in the presence of air, with the organic phase in contact with nitric acid of varying concentration (0.5–4 M) to emulate relevant operational scenarios. The dose rate was estimated to be approximately 3 kGy/h at the time of the irradiation based on a previous dose-rate measurement and decay correction. Cumulative absorbed doses up to 300 kGy were applied. In addition to DBOA solvent (40 vol. % + 25 mM $CyMe_4$-BTBP) and TBP solvent, the pristine organic components were also irradiated at selected doses for comparison.

Following the irradiation, the organic phase was separated and immediately used in extraction tests to assess performance retention and kinetics changes and characterized by spectroscopic and chromatographic methods to probe degradation.

4.4 Analysis

^{241}Am and ^{152}Eu were quantified using High Purity Germanium γ-spectrometry (HPGe; GEM23-195, Canberra) by counting fixed 100 µL aliquots from each phase, using the 59.5 keV peak for ^{241}Am and 121.8 keV peak for ^{152}Eu.

^{237}Np, ^{239}Pu, and ^{244}Cm distribution ratios were determined by α-spectrometry (Ortec, Alpha Duo). Sample preparation was performed by depositing 10 µL aliquots onto planchettes using an acetone-based spreading solution (Z 100), followed by evaporation using IR-light then burn to remove of residual organic matter before counting to adequate peak statistics.

The aqueous phase was also analyzed by ICP–MS (Thermo Fisher Scientific) after significant dilution (reported dilution factor 10^4 in 0.5 M suprapur HNO_3) to quantify actinides (^{238}U, ^{239}Pu, ^{237}Np) and selected inactive elements; indium, scandium, and bismuth were used as internal standards. Non-radioactive samples were additionally analyzed by ICP–OES (Thermo Fisher iCAP 6000 series) using bismuth as internal standard

All reported D ratios were based on triplicate contacts; uncertainties are reported as standard deviations of these triplicate contacts

5. Results and Discussion

As mentioned earlier, several different Chalmers solvents have been developed over the years. This section aims at investigating the system (DBOA – $CyMe_4$-BTBP and FS-13) with the aim to compare it to the system (TBP + $CyMe_4$-BTBP and FS-13).

5.1 Actinide Extractions and An/Ln Separations

The results presented in this section are based on Paper I. The monoamide extractant was first evaluated for its suitability in actinide extraction and for its selectivity toward actinides over lanthanides in an FS-13 diluent system. For comparison, the extraction behavior was benchmarked against the 10% TBP_CHALMEX solvent composition proposed in previous work aimed at improving the hydrodynamic performance of the process.[80] The experiments were performed as described in Section [4.2], and the corresponding data are presented in (Figure 11), where the actinides are efficiently extracted from 3 M nitric acid. Moreover, a clear separation from the lanthanides is observed. In this study, europium was selected as a representative lanthanide. The concentration of $CyMe_4$-BTBP was maintained at 25 mM for all experiments.

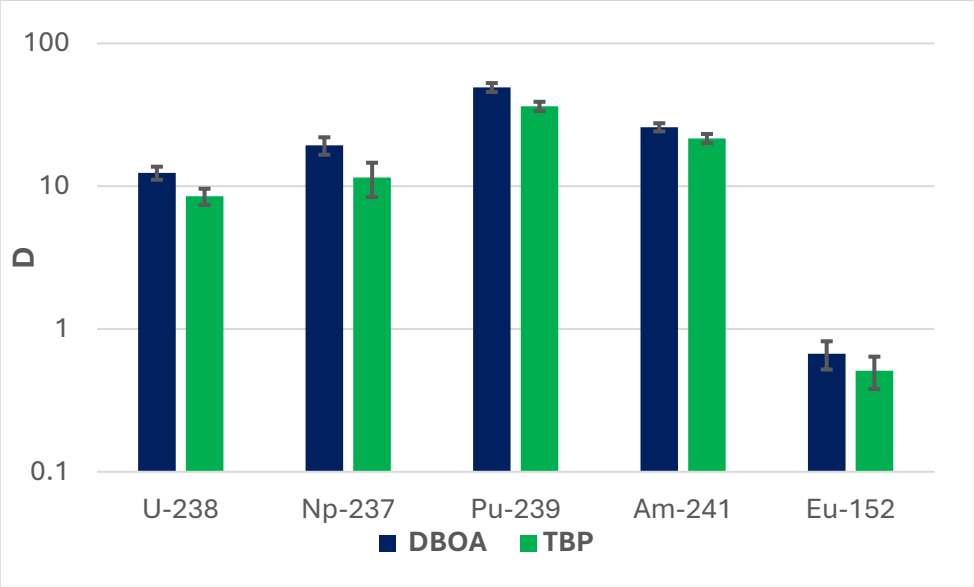

Figure 11. Extraction distribution ratios of actinides and Eu: DBOA vs TBP

The extraction behavior was comparable to that of TBP, so the extraction mechanism was evaluated using slope analysis at 3 M HNO_3 using UO_2^{2+} and Pu^{4+} individually (trace conditions) to avoid competitive effects. The DBOA concentration varied from 10 to 70 Vol%. Log D was plotted versus log [DBOA] (mol L^{-1}). The activity coefficients in the organic phase were assumed to be unity.

As shown in (Figure 12), the slopes are 1.9 for U(VI) and 1.6 for Pu(IV). The uranium slope indicates ~2 DBOA molecules per extracted complex, consistent with solvated nitrato species.

The lower plutonium slope suggests mixed stoichiometries (coexistence of 1:1 and 1:2 species) over the investigated range.

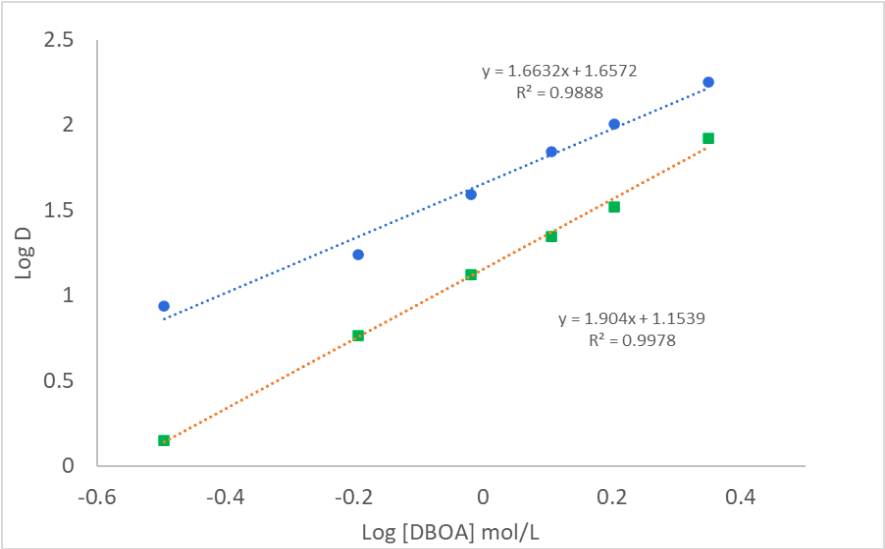

Figure 12. Distribution ratio for uranium and plutonium as a function of log [DBOA] mol/L. Organic Phase: FS-13 + DBOA

The equilibrium expressions for the extraction can be represented by the following equations:

$$UO_2^{2+}{}_{aq} + 2\,NO_3^-{}_{(aq)} + 2\,DBOA_{(org)} \rightleftharpoons UO_2(NO_3)_2.2DBOA_{(org)} \quad (13)$$

$$Pu^{4+}{}_{(aq)} + 4\,NO_3^-{}_{(aq)} + 2\,DBOA_{(org)} \rightleftharpoons Pu(NO_3)_4.2DBOA_{(org)} \quad (14)$$

$$Pu^{4+}{}_{(aq)} + 4\,NO_3^-{}_{(aq)} + DBOA_{(org)} \rightleftharpoons Pu(NO_3)_4.DBOA_{(org)} \quad (15)$$

5.2 Solvent optimization

The aim of solvent optimization in this work was to identify a solvent composition that provides high distribution ratios for the target metal ions while enabling the separation to be achieved with the minimum practical number of extraction stages. To this end, a series of DBOA/FS-13 volume ratios was investigated while maintaining a constant CyMe4-BTBP concentration of 25 mM as an initial optimization step. The distribution ratios of Am(III) and Eu(III) showed a slight increase with increasing DBOA content. However, their extraction is still primarily controlled by CyMe4-BTBP, since monoamides such as DBOA have limited affinity for trivalent actinides and lanthanides in nitrate media.[81] The small increase in D may instead reflect improved solubility/stability of the CyMe4-BTBP–Am/Eu complexes in the mixed DBOA/FS-13 solvent, consistent with reports that lower diluent charge density enhances these properties, and in line with trends observed in TBP-based systems. [66]

For Np, no systematic trend with DBOA/FS-13 composition was observed, as also reported for TBP systems. [66] This is likely due to neptunium redox instability: Np(V) is poorly extractable compared with Np(IV) or Np(VI), and partial reduction of Np(VI) to Np(V) would diminish extraction and mask composition effects.[82]

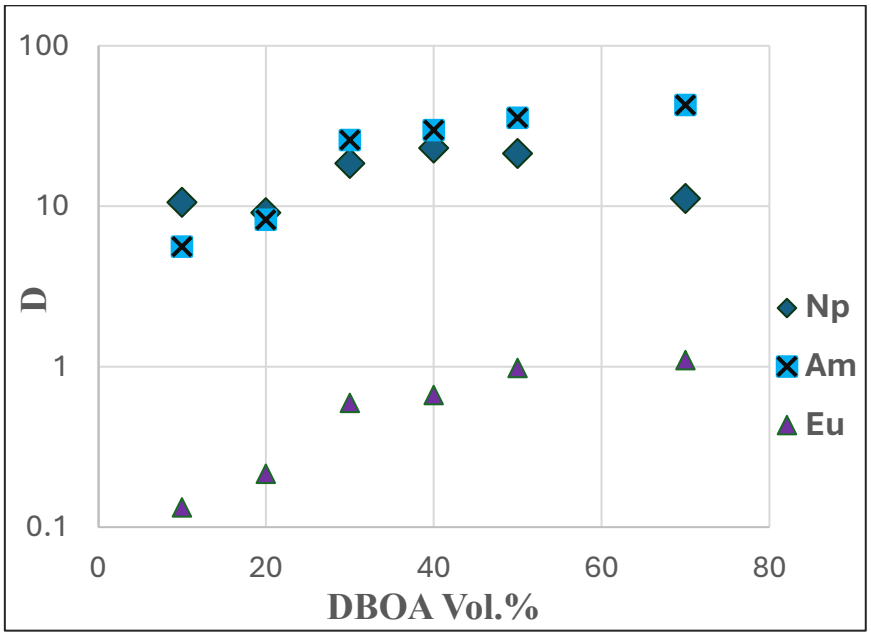

Figure 13. Distribution ratio for neptunium, americium and Europium as a function of [DBOA] Vol.%. Organic Phase : FS-13 + DBOA + $CyMe_4$-BTBP

To determine whether the increased distribution ratios of Am(III) and Eu(III) observed in the mixed DBOA/FS-13 solvent arise from synergistic extraction or from a solvent-matrix effect, mainly to increase the solubility, UV–Vis spectroscopy was used to probe the coordination environment of the extracted complex under representative conditions, using Nd(III) as an optically active surrogate. The resulting spectra (Figure 14) showed no shift in the characteristic Nd^{3+} f–f transitions upon addition of DBOA, indicating that the primary coordination sphere of Nd(III) in the organic phase remains unchanged, and supports the interpretation that the higher *D* for Am(III) and Eu(III) are mainly due to improved solubility/solvation (and thus stabilization) of the extracted $CyMe_4$-BTBP complexes rather than a change in extraction mechanism.

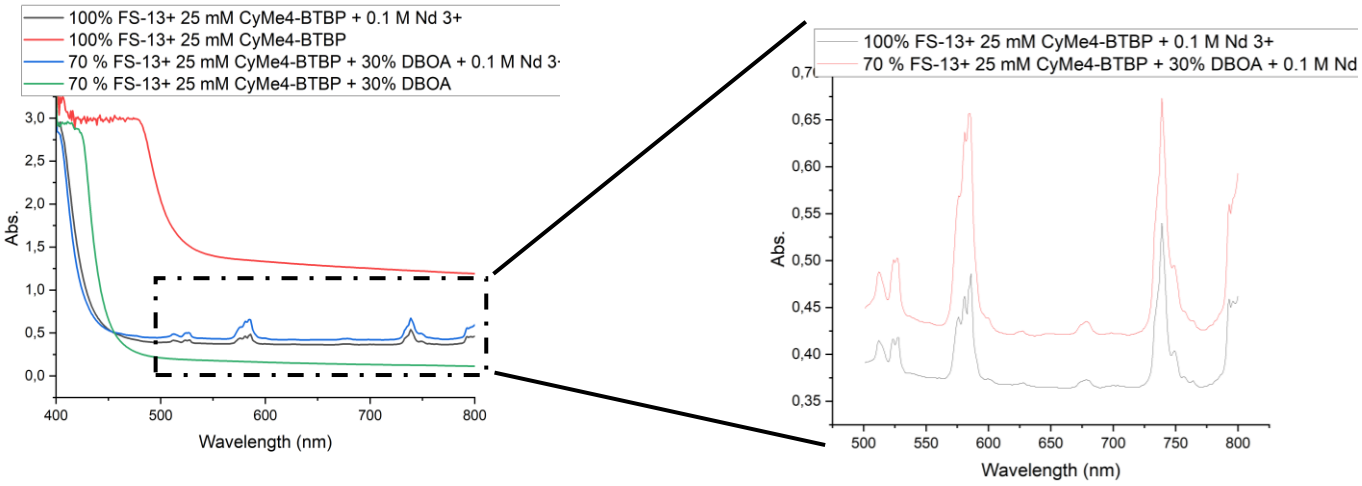

Figure 14. UV–Vis spectra of Nd(III)–CyMe$_4$-BTBP complexes in FS-13 and FS-13/DBOA 30%vol., showing unchanged Nd^{3+} f–f transitions upon addition of DBOA.

5.3 Nitric Acid Dependency

The effect of nitric acid concentration on metal extraction was investigated (Figure 15). As acidity increased, the distribution ratios of U(VI) and Pu(IV) increase systematically, consistent with nitrate-driven extraction: higher HNO_3 increases the availability of NO_3^-, promoting formation of extractable nitrate complexes. In the DBOA system, the dominant extracted adducts are typically described as $UO_2(NO_3)_2 \cdot 2DBOA$ for uranium, and as $Pu(NO_3)_4 \cdot 2DBOA$ and $Pu(NO_3)_4 \cdot DBOA$ for plutonium, reflecting the requirement for two and four nitrate ligands, respectively. At relatively low aqueous acidities, coordination occurs primarily via the amide carbonyl group, and the amide acts as a neutral extractant. As acidity increases, non-ideal behavior can arise due to interactions between free ligand and the extracted metal complex. At sufficiently high nitric acid concentrations, the extraction mechanism may shift from neutral solvation to an anion-exchange pathway. [74]

For trivalent actinides, extraction is governed by CyMe$_4$-BTBP through formation of a 1:2 complex, commonly represented as $[Am(CyMe_4\text{-}BTBP)_2(NO_3)]^{2+}$, which is charge-balanced by outer-sphere nitrate anions, in line with previous reports.[81] Notably, increasing HNO_3 beyond ~5 M led to reduced extraction of Am/Eu (and similarly behaving trivalent species), suggesting that very high acidity begins to suppress extraction, likely through increased acid co-extraction or changes in aqueous speciation and decreased free ligand concentration due to increase protonation of CyMe$_4$-BTBP.[83]

This resembles the behavior of TBP-based systems, where D for trivalent metals decrease above ~2.5 M HNO_3, although the onset occurs at higher acidity in the DBOA system (Figure 15). This shift is consistent with weaker HNO_3 co-extraction by monoamides compared with TBP, due to the higher basicity/polarizability of the phosphoryl (P=O) group relative to the amide carbonyl (C=O), while FS-13 itself has been reported to show negligible HNO_3 extraction.

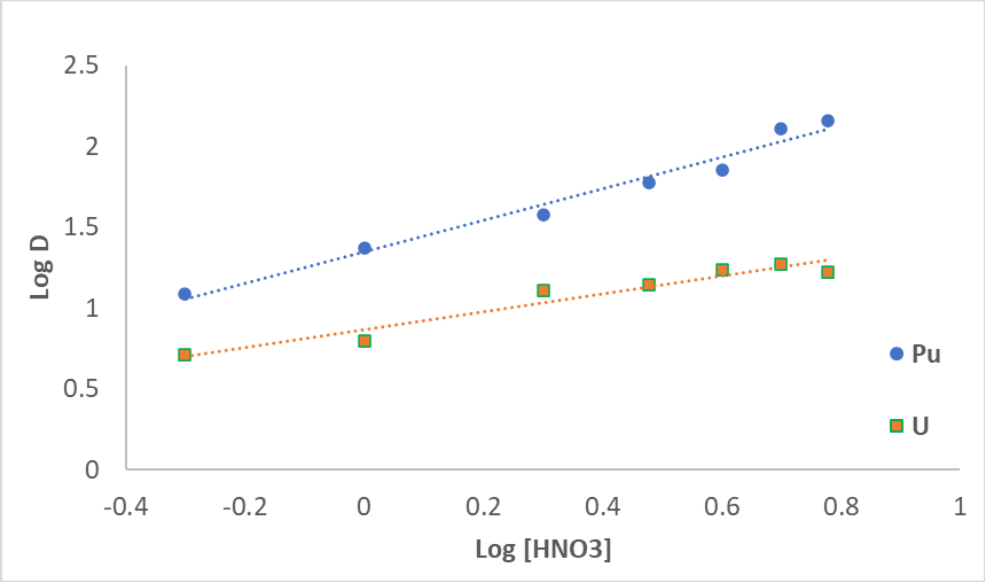

Figure 15. Acidity dependence of U and Pu extraction: log D as a function of log [HNO_3].

5.4 Fission products behavior

Selective actinide recovery in the CHALMEX process must be accompanied by effective rejection of fission and corrosion products to achieve the required decontamination factors. Therefore, the behavior of key impurity surrogates was evaluated in simulated raffinate using DBOA and TBP based solvents while varying the extractant content from 10 to 30 vol.% (DBOA: 0.34–1.01 M; TBP: 0.37–1.11 M). The results (Figure 16) show that approximately half of the investigated elements exhibit low extractability ($D < 0.1$), which is favorable for minimizing co-extraction; however, several elements showed higher distribution ratios and may become process-relevant, particularly when their inventories in spent fuel are high. In general, increasing the extractant content increased D for many fission/corrosion products, consistent with a greater availability of coordination sites in the organic phase.

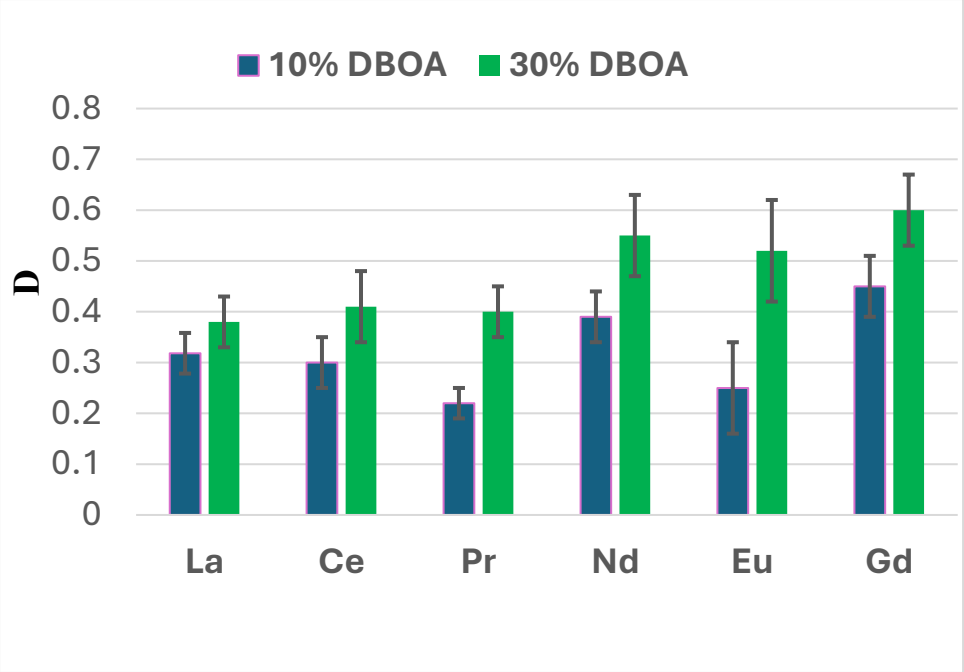

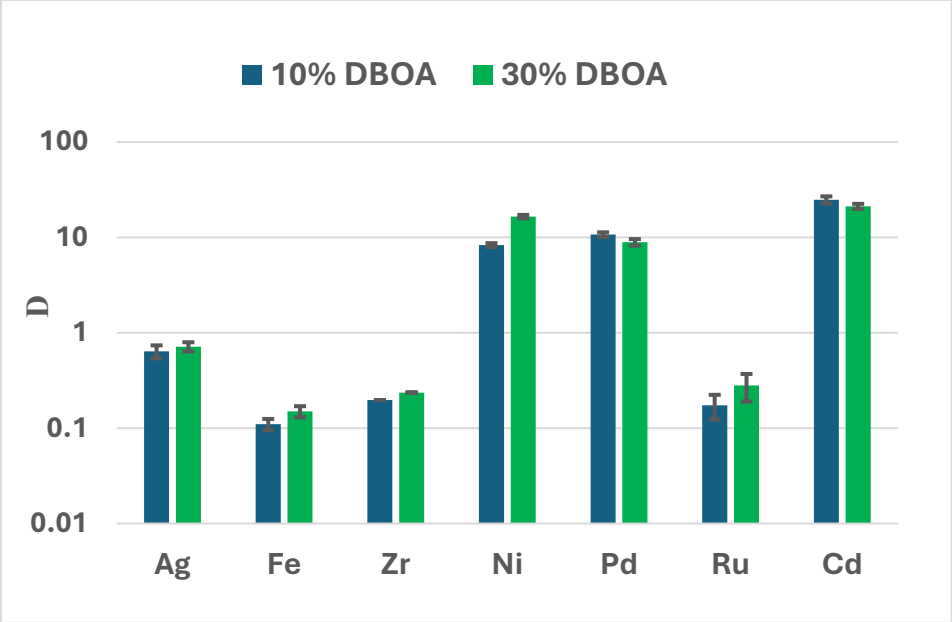

Figure 16. Effect of DBOA concentration on distribution ratios of lanthanides and selected impurities

Lanthanides showed moderate extraction (D ≈ 0.2–0.6) with a gradual increase from La to Gd, consistent with the lanthanide contraction. DBOA gave slightly higher D than TBP for the lighter lanthanides (La–Pr), while the differences diminished for the heavier lanthanides (Nd–Gd), in line with reports that monoamides can extract lanthanides somewhat more strongly than TBP. From a process perspective, iron is particularly important because of its high abundance in spent fuel (~1500 ppm). However, iron is not a fission product. It mainly originates from corrosion and the partial dissolution of stainless steel during nitric acid dissolution. In the DBOA system iron remained weakly extracted relative to TBP, but a clear contact-time dependence was observed. D(Fe) increasing from ~0.07 to ~0.15 after 20 min. A similar

behavior was observed for Ni, indicating that shorter residence times during mixing/settling could further improve decontamination from these slowly transferring elements. Finally, the application of masking agents (0.2 M D-mannitol and 20 mM Bimet) effectively suppressed problematic elements (Zr, Mo, Pd) following established approaches. Under these conditions Zr and Pd were reduced below detection limits and Mo decreased markedly (e.g., D ≈ 2.62 to 0.016 in the DBOA system), with comparable suppression observed in both DBOA and TBP solvents. Overall, the data indicates that DBOA offers TBP-comparable impurity handling while highlighting practical optimization levers, namely residence-time control and targeted masking, to manage the elements most likely to drive decontamination performance in a flowsheet.

5.5 Solvent stability

The radiolysis and hydrolysis stability were performed according to the section [4.3.1]

5.5.1 Hydrolysis stability

The aim of this experiment is to evaluate the effect of nitric acid on the stability of the organic solvent during prolonged contact with an aqueous phase. Under conditions representative of solvent extraction operations, establishing the hydrolytic stability of the solvent system is essential.

In summary, the hydrolytic behavior of the DBOA-based solvent system appears to be relatively robust for all actinides investigated. This contrasts with earlier work on DEHBA in cyclohexane, where the americium distribution ratio decreased steadily after extended contact times. That decrease was attributed to the formation of water-soluble degradation products from DEHBA, which suppressed extraction. [84]

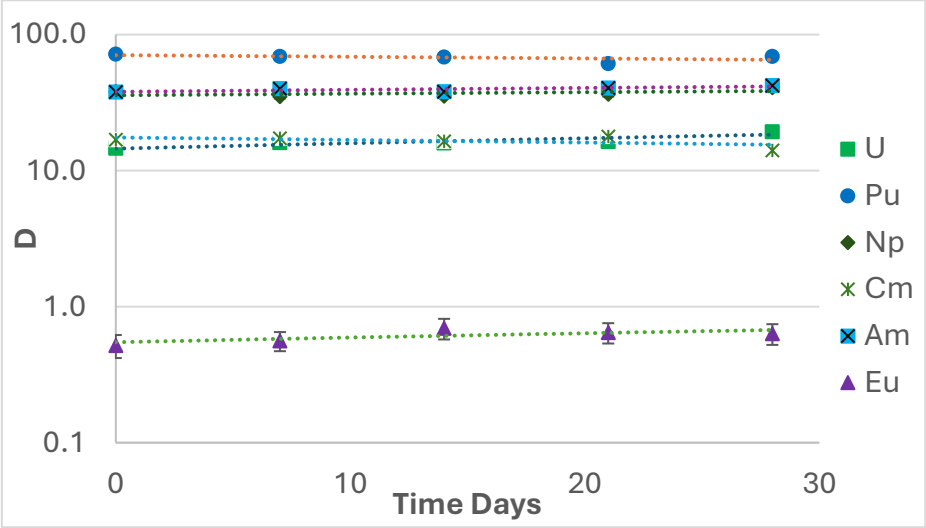

Figure 17. Distribution ratios for actinides and ^{152}Eu as a function of time during the hydrolytic stability study. Dishlines are trend lines

Compared with the previously studied TBP solvents[85], the DBOA system shows a similar trend, likely driven by the diluent. The data also shows a steady distribution ratio during the whole

experiment. In this way, the acidic aqueous phase may act as a scavenger, like how the aqueous phase scavenges radicals during irradiation experiments.[76]

5.5.2 Radiolysis Stability

As described in Section [4.3.1] the experimental procedure for the irradiation tests is the same for all samples. In this section, two sets of results from the γ-irradiation experiment are shown.

One of the main motivations for replacing TBP is that its radiolysis can generate undesirable degradation products. In contrast, the radiolysis products expected from DBOA are generally considered more benign, primarily carboxylic acids, amines and amides. For that reason, radiolytic stability is an important parameter to assess, since it gives an overall picture of how the solvent system behaves under irradiation.

For the first dataset, the organic phase was irradiated up to 300 kGy, then extraction performance was tested with an aqueous phase containing only actinides (without the complex matrix of fission and corrosion products). The corresponding distribution ratios are shown in (Figure 18).

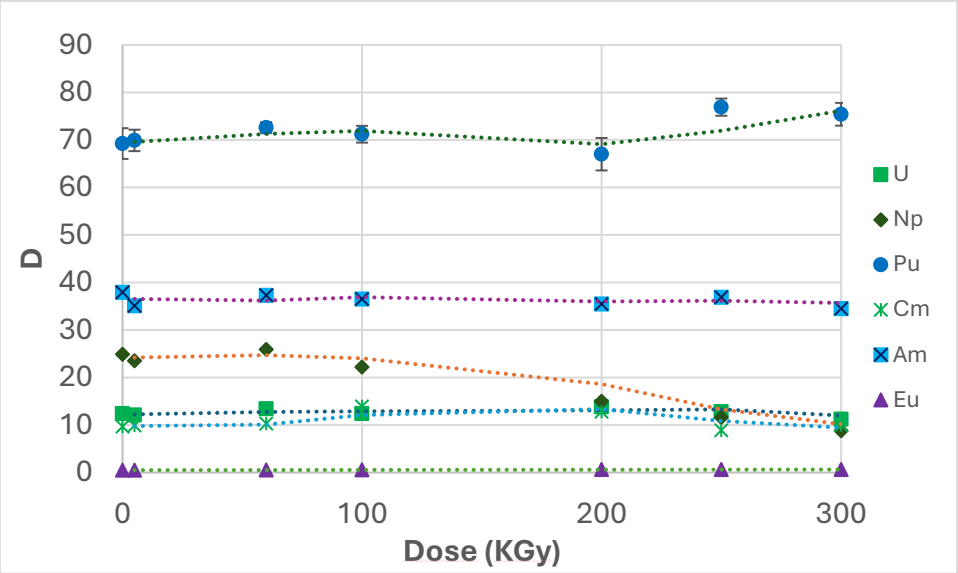

Figure 18. Effect of γ-irradiation dose (0–300 kGy) on the distribution ratios of selected actinides and europium-152. Aqueous phase: 3 M HNO_3 solution containing radionuclides.

Overall, the distribution ratios show different trends with increasing absorbed dose. U, Pu, Am, and Cm remain relatively stable over the full dose range, whereas Np shows a clear decrease in extractability as the dose increases.

This decline in neptunium extractability is likely linked to long-lived reactive species produced during irradiation, which can drive redox changes between Np(VI) and Np(V). This interpretation is consistent with earlier study on neptunium redox chemistry in 4 M HNO_3 under γ-irradiation, where UV–Vis spectroscopy was used to track redox-speciation. With continued irradiation, as nitrous acid accumulates in solution, Np(VI) is progressively reduced back to

Np(V), which is known as less favorable to extract. This would explain the reduces of Np extraction performance.[86]

Literature reports that the net reduction of Np(VI) is observed only after nitrous acid (HNO_2) has accumulated to a sufficiently high concentration in the system

$$\text{Np(VI)} + \text{HNO}_2 \rightarrow \text{Np(V)} + NO_2^{\bullet} + H_{aq}^{+} \qquad (16)$$

The second dataset was performed to evaluate the matrix effect, where the aqueous phase simulated a synthetic spent nuclear fuel solution. The study covered the same absorbed-dose range. In this section, the maximum dose investigated so far in our work, 300 kGy, is discussed. At this absorbed dose, the physical appearance of both the organic and aqueous phases changed after the irradiation. (Figure 19) shows the aqueous and organic phases before and after irradiation at 300 kGy.

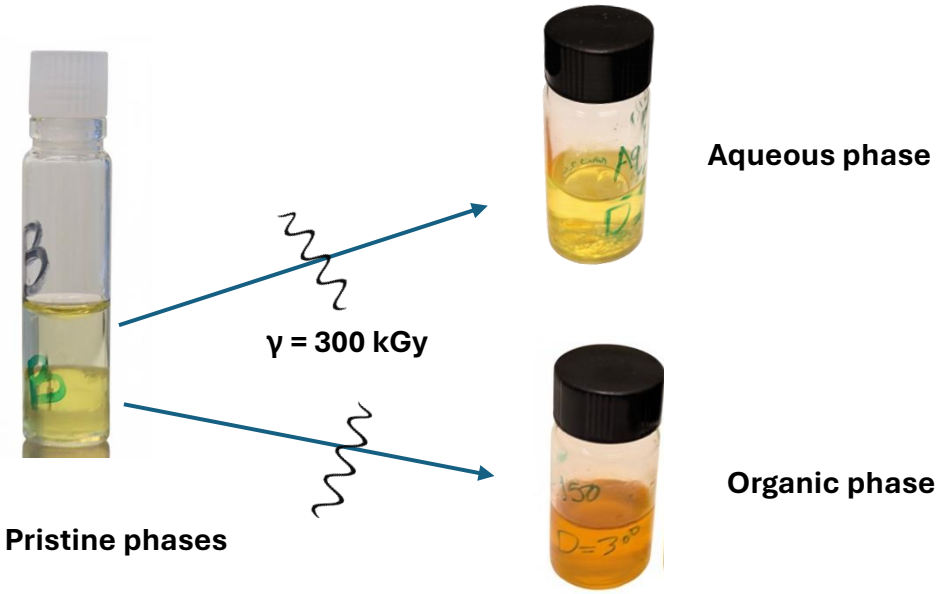

Figure 19. Visual appearance of the aqueous and organic phases before (pristine) and after γ-irradiation at an absorbed dose of 300 kGy.

The extraction data for this condition is shown in (Figure 20) A clear decrease in the distribution ratios was observed for all actinides. In contrast, the fission products did not show any meaningful trend that could explain this decrease. Since this behavior was not observed in the absence of fission products, further investigations were carried out. Moreover, given the obvious changes in the solvent's physical properties after irradiation, it is possible that the system kinetics were also affected.

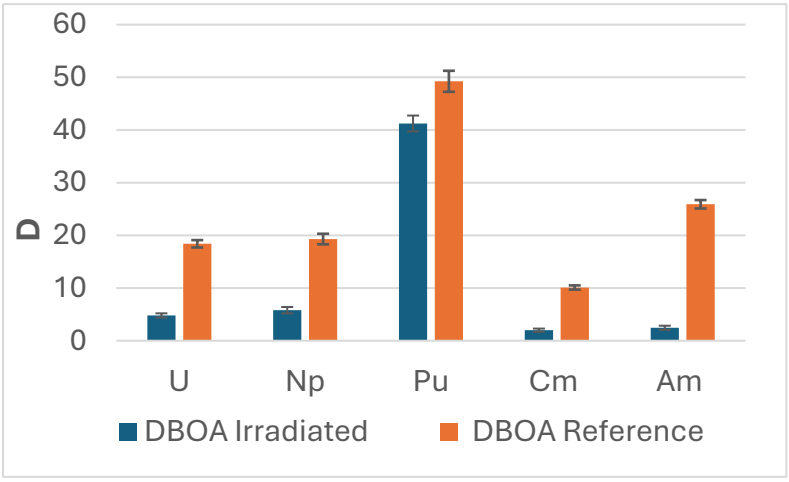

Figure 20. Distribution ratios of actinides using DBOA solvent, comparison between reference and gamma-irradiated (300 kGy) solvent systems. Extraction contact time:75 min, aqueous phase: simulated raffinate solution containing radionuclides

To address this performance and compensate for the apparently slower extraction kinetics in the irradiated raffinate case, the contact time was increased to 90 min. As summarized in (Figure 21) this adjustment resulted in a partial recovery of extraction efficiency, yielding values comparable to those of the unirradiated system. Extending the contact time to 120 min led to a reduction in the D for Am and Np.

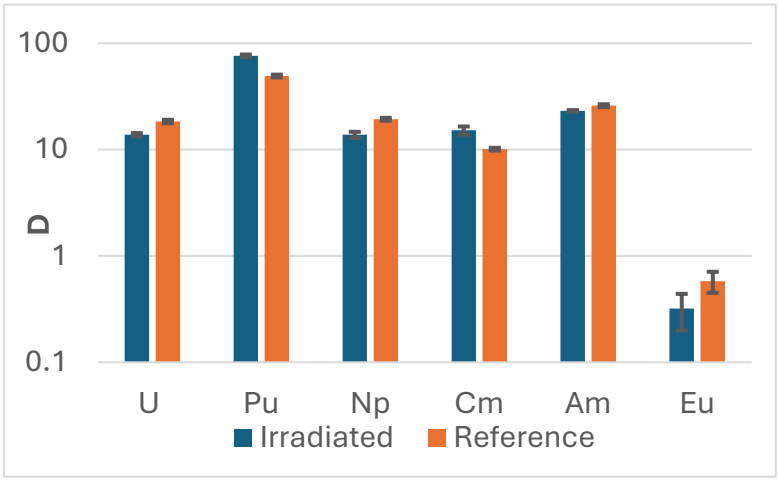

Figure 21. Distribution ratios of actinides and europium-152 using DBOA solvent, comparison between reference and gamma-irradiated (300 kGy) solvent systems. Extraction contact time:90 min, aqueous phase: simulated raffinate solution containing radionuclides

For the trivalent elements, only minor variations were observed, with a slight increase for Cm and a small decrease for Eu. Such trends have been attributed to the formation of irradiation products in FS-13 that act as stronger extractants than the parent ligand.[87] For neptunium, the reduced extractability is plausibly explained by the presence of radiolysis products such as $HONO/NO_2$ species, which can modify Np redox speciation toward less extractable forms.

The pronounced changes in phase appearance observed after γ-irradiation are consistent with radiolysis generating degradation products (e.g, nitrous acid) that alter the solvent's physicochemical properties, including viscosity, density, and interfacial behavior. These changes can favor the formation of interfacial films and increase viscosity, thereby reducing diffusion and slowing interfacial mass transfer. [88] Consequently, longer phase-contact times may be required for the irradiated system to approach distribution equilibrium. Literature reports that absorbed dose can measurably alter the hydrodynamic properties of FS-13–based solvent mixtures, viscosity was reported to increase progressively with increasing absorbed dose.[89]

5.5.2.1 Investigation of radiolysis products

To better understand the irradiation behavior of the solvent at an absorbed dose of 300 kGy, both the pristine extractant and the solvent were irradiated in contact with 3 M nitric acid. After irradiation, the solutions were analyzed using GC–MS, FTIR, and UV–Vis spectroscopy.

The GC–MS chromatograms are shown in (Figure 22, 23) comparing pristine and irradiated DBOA, FS-13, and the DBOA solvent system. No differences in the peak pattern were observed, and no new impurity peaks appeared. This indicates that, within the detection limits of the instrument, no radiolysis products were detected. In addition, the relative peak ratios remained similar, suggesting that no significant decomposition occurred under these conditions. In the solvent chromatograms two dominant peaks are observed: the first at ~4.2 min, assigned to FS-13, and the second at ~9.1 min, assigned to DBOA. After irradiation, the chromatogram shows the same two peaks with no additional peaks.

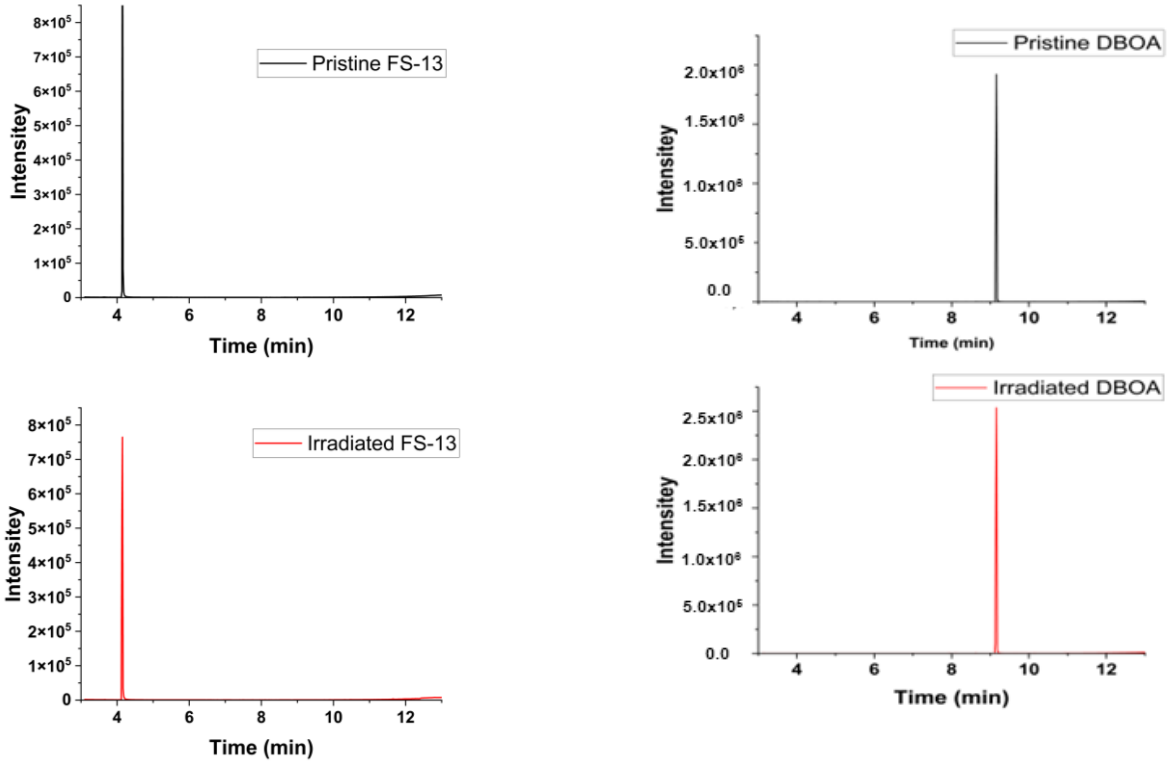

Figure 22. GC–MS chromatograms of FS-13 (left) and DBOA (right) before (pristine) and after γ-irradiation (300 kGy).

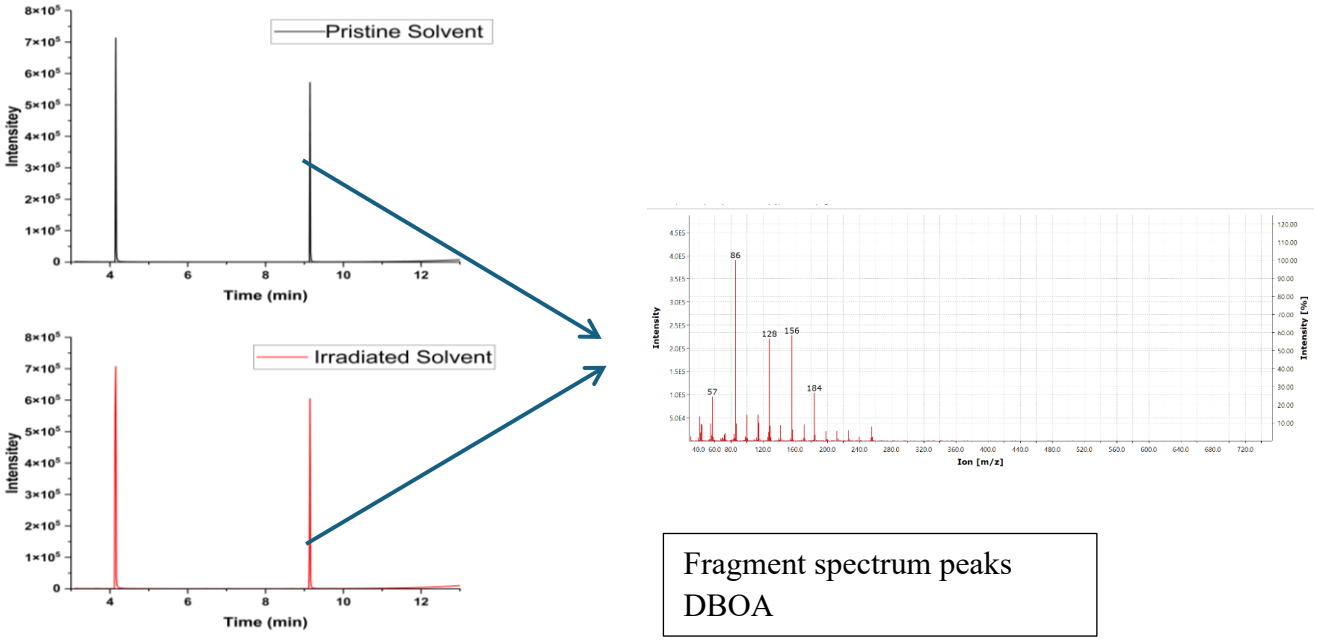

Figure 23. GC–MS chromatograms of the DBOA/FS-13 solvent system before (pristine) and after γ-irradiation (300 kGy), with the corresponding EI–MS fragment spectrum of the DBOA peak.

GC–MS analysis confirmed that the main compound remained intact, with no significant degradation products detected within the measurement range. This suggests that any radiolysis products, if formed, are present only at trace levels below the instrument's detection limit. However, even trace amounts of degradation products may influence the extraction behavior, since the experiments were performed with actinides at trace concentrations. To further support these observations, FTIR spectroscopy was also performed, and the corresponding spectra are presented in the following figures.

The FT-IR spectra of FS-13 seen in (Figure 24), before and after irradiation up to an absorbed dose of 300 kGy, showed no observable changes in peak positions, intensities, or band shapes. The spectral profiles were virtually identical across the full wavenumber range (4000–500 cm^{-1}), indicating that FS-13 is highly resistant to radiolytic degradation under the experimental conditions.

This stability aligns with the known chemical robustness of the FS-13 perfluorinated diluent. [43]

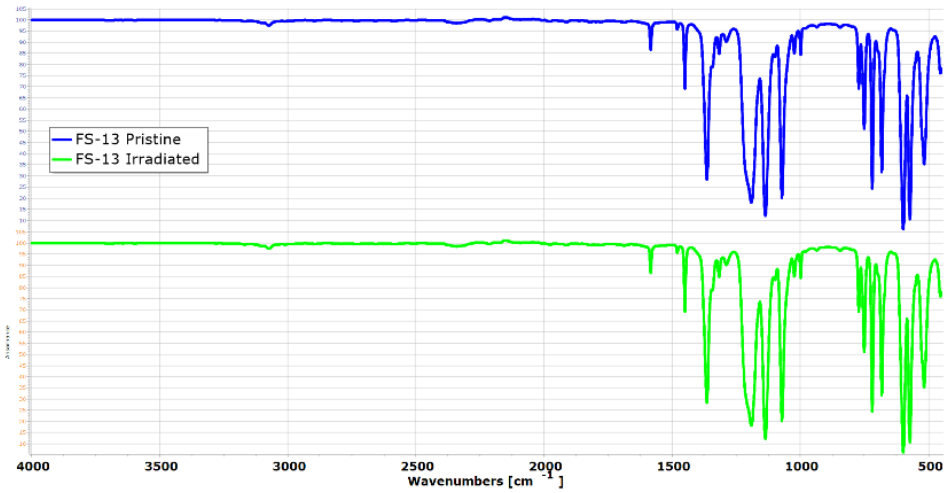

Figure 24. FTIR spectra of FS-13 before and after irradiation

When comparing the FT-IR spectra of neat pristine DBOA and the γ-irradiated sample (Figure 25), significant spectral changes are observed after irradiation. Notably, an additional absorption band appears at ~1715 cm^{-1}, attributed to C=O stretching of newly formed carbonyl-containing degradation products (consistent with oxidative degradation; potentially including carboxylic-acid-type products). The intense band in the ~1630 cm^{-1} region is present in both spectra and corresponds primarily to the amide I (C=O) vibration of DBOA. In the fingerprint region (1400–800 cm^{-1}), increased congestion and band broadening after irradiation suggest the formation of a mixture of degradation products (e.g., alkyl fragments and oxygenated/nitrated species).

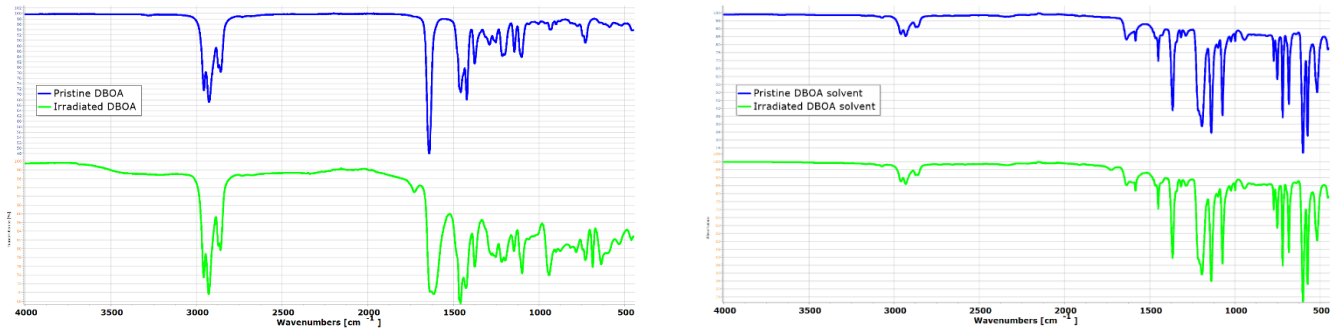

Figure 25. FTIR spectra of (left) DBOA , (right) DBOA solvent before and after irradiation

The DBOA-based solvent system showed, in the fingerprint region, slight broadening and a reduction in peak intensity. This suggests partial degradation of the amide group due to radiolytic cleavage. Furthermore, the appearance of a new absorption band at 1715 cm^{-1} in the irradiated sample is consistent with C=O stretching vibrations. These are characteristics of saturated aliphatic carbonyl compounds, indicating the formation of new degradation products. Overall, the DBOA based solvent system exhibited significantly improved radiolytic stability compared to neat DBOA when subjected to an equivalent absorbed dose of 300 kGy. This enhancement is primarily attributed to the dilution effect. Lowering the local concentration of DBOA molecules reduces the likelihood of radical induced degradation. Additionally, the use of FS-13 as the diluent contributes to the system's stability due to its inherent resistance to radiolytic decomposition. This resistance stems from the strength of C–F bonds and low reactivity under ionizing radiation.

Further investigation is required to identify the specific radiolysis products responsible for the changes in system kinetics and to assess whether post-irradiation solvent-washing protocols can effectively mitigate their impact. Preliminary UV–Vis measurements of FS-13 and the DBOA-based solvent, pre-equilibrated with 3 M HNO_3 and subsequently irradiated to an absorbed dose of 300 kGy, revealed new absorption features in the 350–450 nm range. These bands are consistent with the presence of $HONO/NO_2$ species, which are well-known radiolysis products of nitric acid. Their transient partitioning into the organic phase may contribute to the observed alterations in extraction kinetics. Consequently, implementing a systematic washing step should enable the removal of these species and improve solvent performance.

5.6 Batch Flowsheet

This section is based on data from Manuscript II. To evaluate the feasibility of replacing TBP with DBOA in the CHALMEX process, a batch flowsheet was tested, consisting of extraction, scrubbing, and stripping steps. All tests were performed in the presence of a masking agent and under metal-loading conditions representative of the full fission-product matrix, as described in Section [4.2].

5.6.1 Scrubbing stage

Following extraction, the scrubbing stage was applied to the loaded organic phase with two main objectives: reduce co-extracted nitric acid, and remove accompanying metal impurities, while maintaining actinide loading. In solvating extractant systems such as TBP and monoamides DBOA, nitric acid is co-extracted to varying extents; consequently, scrubbing conditions must be selected to remove acid without promoting undesired actinide back-extraction.

Scrubbing was performed at O/A = 1 using 0.5 M HNO_3 as a baseline, followed by a nitrate-activity series in which $NaNO_3$ (0.5–3.5 M) was added while maintaining constant acidity (0.5 M HNO_3). Previous scrub solution reported was 0.5M HNO_3. This design separates the effect of nitrate strength from acidity.

Increasing nitrate activity is expected to stabilize neutral nitrate solvates in the organic phase thereby suppressing actinide back-extraction during scrubbing, while maintaining sufficiently low free acidity to facilitate removal of co-extracted HNO_3. The scrubbing stage was also evaluated from an operational perspective, since inappropriate conditions can increase the risk of third-phase formation, emulsions, slow phase disengagement, and crud generation, particularly under high acid/metal loading.

Actinide retention during scrubbing: TBP vs DBOA

The actinide retention trends observed during scrubbing are consistent with the behavior expected for solvating extractants:

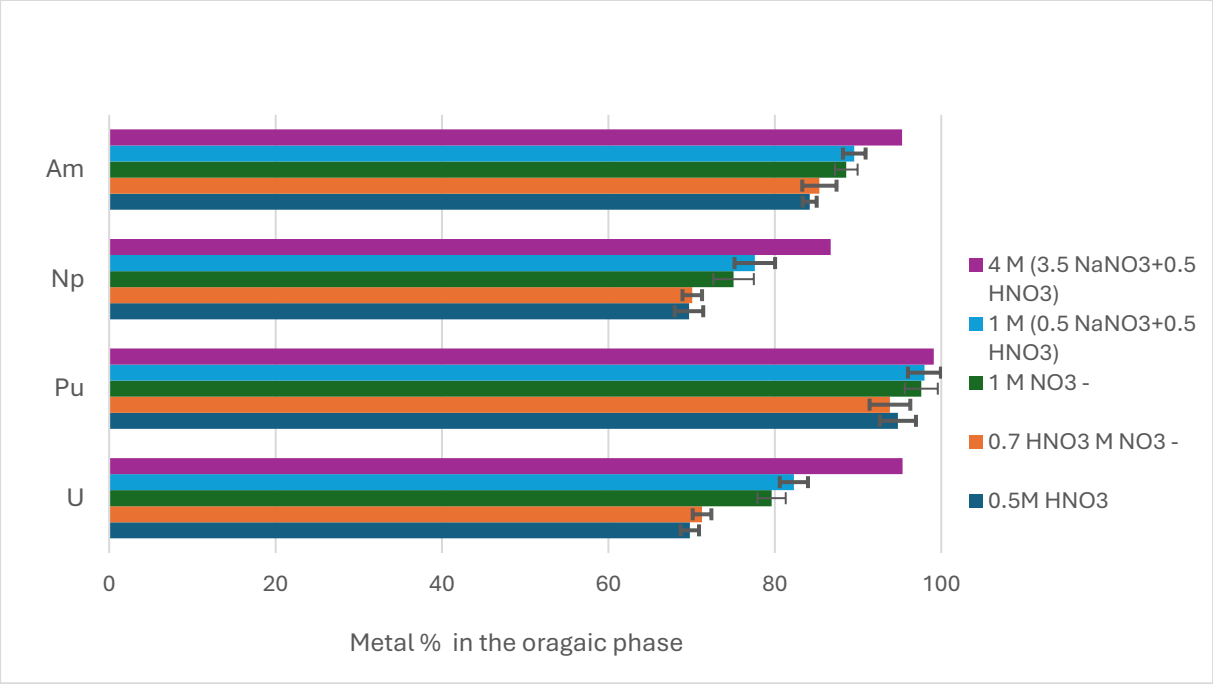

Figure 26. Organic-phase metal fraction for actinides extracted by DBOA using varying scrub solutions.

For DBOA solvent as seen in Figure 26, retention showed a stronger dependence on nitrate strength. Scrubbing with 0.5 M HNO_3 alone produced the lowest retention, most notably for U and Np both less than 70%, indicating increased susceptibility to back-extraction at low nitrate activity. Upon increasing nitrate ($NaNO_3$ + 0.5 M HNO_3) up to the highest nitrate condition shown, the retained fractions of U and Np increased substantially. Pu remained highly retained under all scrub compositions, while Am was strongly retained throughout but improved further at elevated nitrate. This behavior is consistent with nitrate-dependent stabilization of extracted neutral nitrate–ligand species in monoamide systems, commonly described by U(VI) species of the type $UO_2(NO_3)_2 \cdot 2L$

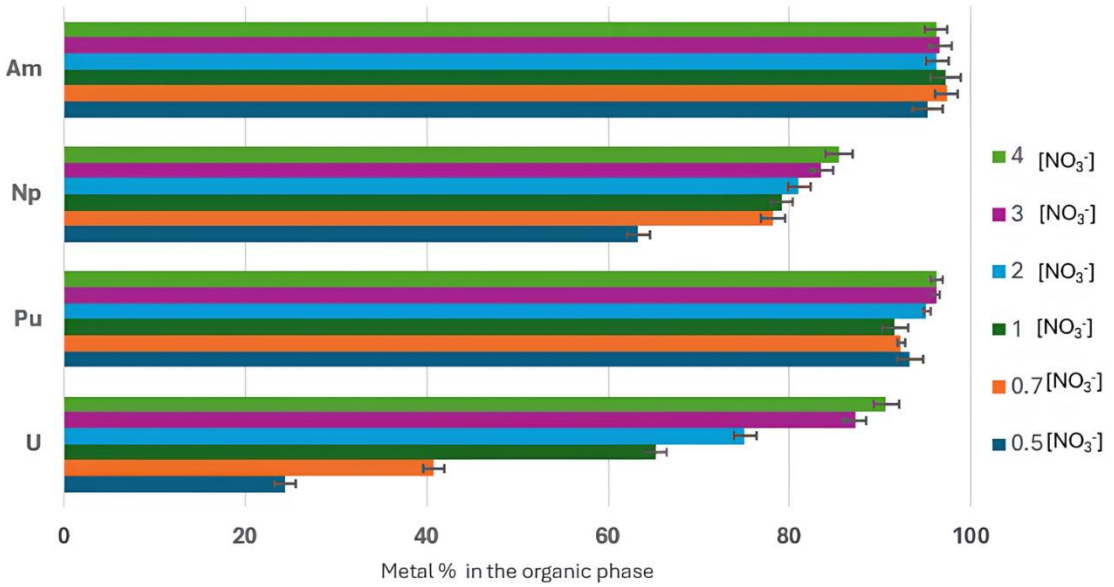

Figure 27. Organic-phase metal fraction (%) for actinides extracted by TBP using varying scrub-solution concentrations (M).

The TBP solvent (Figure 27), increasing the nitrate concentration in the scrub liquor (≈1–4 M NO_3^-) increased retention of U and Np in the organic phase, while Pu and Am remained highly retained over the full range. With a scrub solution of 0.5 M HNO_3, scrubbing was poor, where only 25% of U remained in the organic phase. This is explained by the nitrate-dependent formation of the neutral uranyl complex $UO_2(NO_3)_2 \cdot 2TBP$, increased$[NO_3^-]$stabilizes this species, making U harder to back extract during scrub stage. Eq. 17.

$$UO_2^{2+} + 2\,NO_3^- + 2TBP_{(org)} \rightleftharpoons UO_2(NO_3)_2.2TBP_{(org)} \qquad (17)$$

In contrast, Am(III) extraction by CyMe4-BTBP is governed primarily by strong N-donor complexation and associated ion-pairing, so variations in nitrate concentration typically have a smaller effect on D_{Am}than for U(VI).

$$Am^{3+}_{(aq)} + NO^-_{3_{(aq)}} + 2\,CyMe4\_BTBP_{(org)} \rightleftharpoons [Am(CyMe4-BTBP)_2(NO_3)]^{2+}_{(org)} \qquad (18)$$

Overall, these results identify total nitrate concentration as a key operational variable governing actinide retention during scrubbing, and they show that TBP and DBOA differ in the magnitude of nitrate dependence, with DBOA exhibiting the more pronounced response under the tested conditions. Differences in scrubbing between TBP and DBOA likely arise from nitric acid co-extraction and organic-phase speciation: TBP forms $HNO_3 \cdot$TBP adducts and can take up

significant HNO_3/H_2O, reducing free TBP for metal solvation, whereas monoamide behaves differently, leading to different retention trends.

The influence of nitrate strength on the accompanying metal impurities is illustrated by the lanthanide dataset obtained during scrubbing with $NaNO_3$ + 0.5 M HNO_3.

Table 2. Metal removal % during scrub stage

Scrub composition	La	Ce	Nd	Sm	Eu
0.5 M $NaNO_3$ + 0.5M HNO_3	49.3	32.4	16.5	20.9	16.8
1.5 M $NaNO_3$ + 0.5M HNO_3	53.5	39.6	16.1	23.3	23.1
2.5 M $NaNO_3$ + 0.5M HNO_3	47.6	30.3	14.1	25.1	24.8

In general, varying the scrub-solution composition had only a limited impact on lanthanide decontamination. Across the tested conditions, the scrub step removed roughly 40–50% of the light lanthanides (La, Ce), whereas removal of the heavier lanthanides was lower and remained around ~20–25% (Nd–Eu) per scrub stage.

5.6.2 Strip Stage

In this study three stripping solutions were investigated, while keeping identical extraction and scrubbing steps. The strip solutions were 0.5 M glycolic acid adjusted to (pH ~4) , and diluted nitric acid at two concentrations (0.1 M and 0.01 M HNO_3). Stripping performance was quantified as stripping efficiency (%), and the results for both the TBP and DBOA solvents are presented in Figure 28.

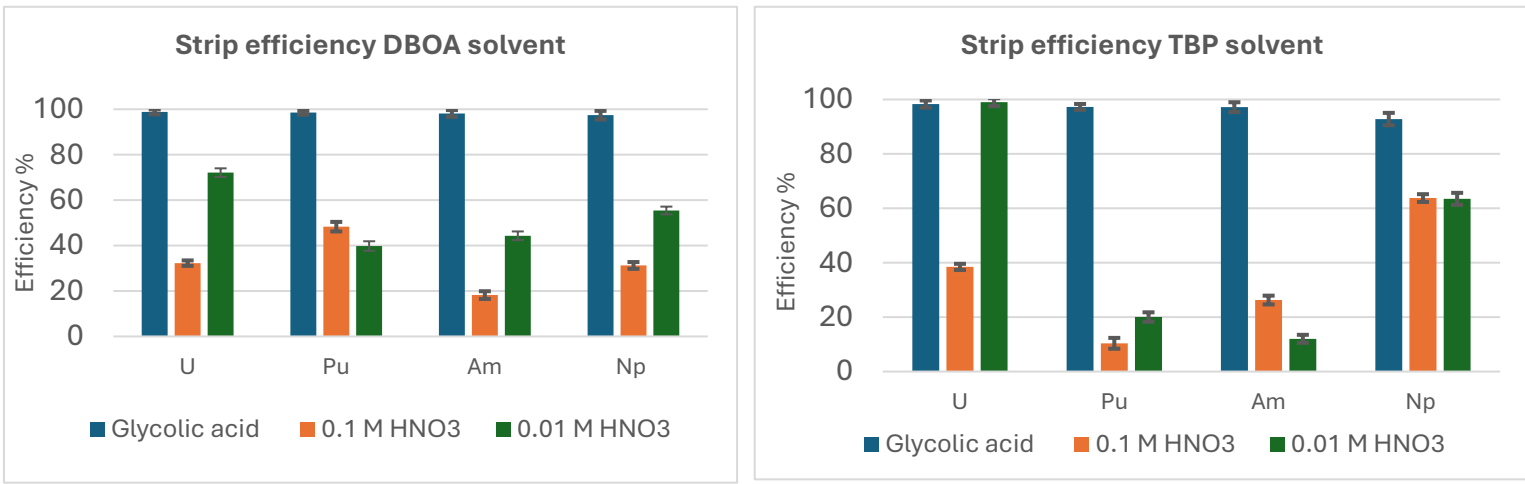

Figure 28. Strip efficiency (%) for actinides from DBOA(left) and TBP(right) organic phases using glycolic acid and dilute nitric acid solutions.

For the glycolic acid solution, the aqueous phase pH was adjusted using NaOH to reach the target value (pH=4) after phase contact. This step is important because a single scrub contact did not remove all co-extracted nitric acid, and the residual acidity carried in the loaded organic phase can directly depress the effective pH during stripping, thereby influencing stripping performance. In a realistic process implementation, however, the organic phase would undergo multiple scrub stages, such that the remaining nitric acid would be sufficiently reduced and its contribution to the strip-stage pH would become negligible.

Overall, the strip-stage results demonstrate that 0.5 M glycolic acid provides near-quantitative back-extraction of U, Pu, Am, and Np from both the DBOA- and TBP-based solvents. The DBOA formulation performed marginally better, with stripping efficiencies typically in the range of 97–99%.

In the nitric acid strip solution, where the particularly high stripping of U from TBP at 0.01 M HNO_3 reflects the nitrate-dependent stability of extracted uranyl–TBP complexes. However, this behavior is not mirrored for Pu and Am, emphasizing that acid adjustment alone cannot ensure total actinide recovery. Under a realistic process scenario, multiple stripping stages would be implemented. Therefore, even if the single-contact stripping efficiency is modest, the actinides can still be quantitatively back-extracted by staging.

Because the scrubbing applied here was not sufficient to remove all co-extracted nitric acid, two nitric acid strip concentrations (0.1 M and 0.01 M HNO_3) were evaluated to assess the sensitivity to residual acidity carried by the organic phase. In a fully optimized flowsheet, where nitric acid is effectively removed through adequate scrubbing, the 0.1 M strip would be expected to perform similarly to 0.01 M HNO_3 at single contact experiment. In the present dataset, the lower-acidity condition generally provided higher recovery, consistent with reduced acid hold-back during stripping.

Consequently, for a CHALMEX-type flowsheet targeting robust actinide product recovery and minimized solvent hold-up, glycolic acid is the preferred strip reagent. However, the comparison of stripping performance for the DBOA- and TBP-based solvent systems was not only conducted to evaluate chemical efficiency of actinide back-extraction, but also to assess the nature of the recovered aqueous product liquor in view of its direct reintegration into the fuel fabrication route. In an industrial recycling context, minimizing downstream conditioning steps is essential, the recovered actinide stream should ideally be produced in a chemical form that is already compatible with established fabrication feed specifications.

Table 3. Percentage of metals back extracted into the aqueous phase during the stripping stage from DBOA and TBP solvents

	DBOA			TBP		
	Glycolic acid	0.01 M HNO_3	0.1 M HNO_3	Glycolic acid	0.01 M HNO_3	0.1 M HNO_3
Sm	13.9	14	9.3	15	1	6
Pm	1.2	2.3	1.6	17.1	20	13.1
Cd	0.2	0.2	0.2	0.4	0.2	0.3
Ni	0.6	0.4	1.4	0.4	0.4	0.4
Fe	0.8	0.7	0.73	0.8	0.7	0.8
Cu	4.1	1.1	12.1	1.1	1.4	6.3

Lanthanides showed only partial transfer to the aqueous phase, as the data in table 3. Approximately 5–15% of the lanthanides, particularly the heavier lanthanides, were stripped. In contrast. For transition metals, less than 1% of the loaded organic inventory of Ni, Cu, Fe, and Cd was transferred to the strip solution.

In summary, the aim of comparing DBOA and TBP stripping with glycolic acid versus nitric acid is to identify a strip strategy that simultaneously ensures high actinide recovery and stable operation and delivers a product liquor as close as possible to the chemical form required for direct reintegration into the fabrication route. In the context of sol–gel fabrication, nitrate product solutions represent the most straightforward option for reintegration into the fabrication route, since they are already aligned with established feed specifications and therefore require fewer additional chemical conversion steps

By contrast, glycolic-acid stripping can provide high recovery and may reduce the number of process steps; however, it yields a non-nitrate product matrix. Sol–gel fabrication would therefore require adjustment to accommodate this solution. Otherwise, precipitation-based powder production may be simpler than sol–gel fabrication, although it would introduce additional downstream challenges.

5.6.3 The DBOA flowsheet

The single-contactor flowsheet (Figure 29) for the DBOA-based solvent system shows promising performance; however, actinide losses and the decontamination factors of the final products should be improved before progressing toward scale-up and counter-current operation. To support this transition, it is particularly important to quantify the total amount of co-extracted nitric acid in the loaded organic phase and the extent of acid removal in each scrub stage, as these parameters influence both extraction efficiency and subsequent stripping behavior.

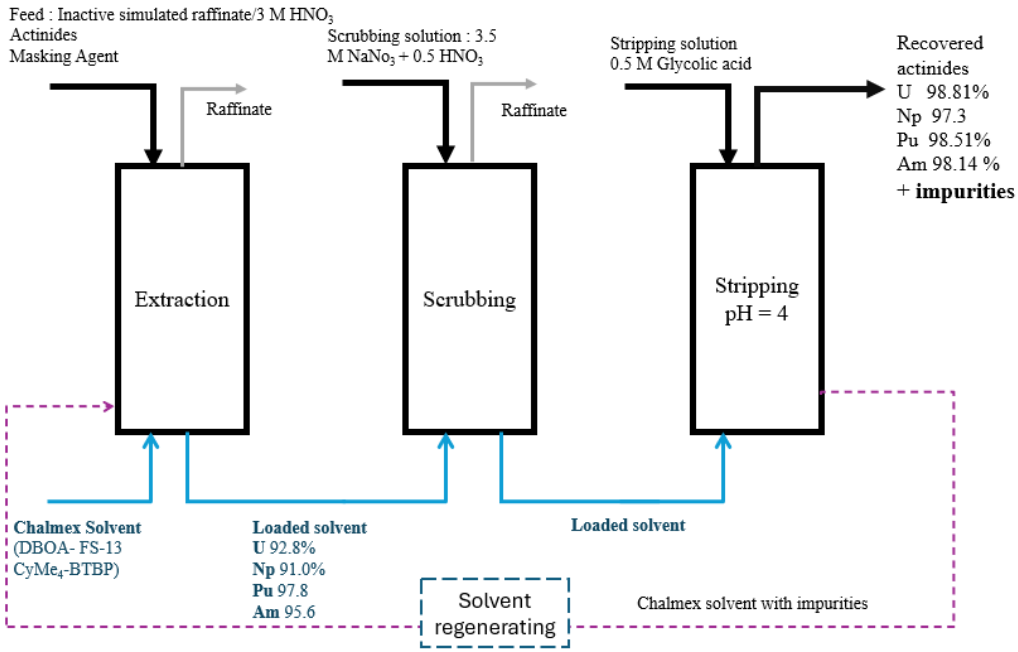

Figure 29. Single-contactor DBOA CHALMEX flowsheet (extraction–scrub–strip).

In the scrubbing section, approximately 20–25% of the lanthanides are removed per scrub stage. Additional scrub stages would be expected to further reduce the carryover of these impurities Under the current conditions, PGMs remain predominantly in the organic phase, and a significant fraction of co-extracted Ni, Cu, and Fe are also retained in the organic phase after scrubbing. To mitigate actinide losses, potential strategies include recycling the scrub solution or alternatively routing the scrub stream back to the feed, depending on the overall mass balance and impurity build-up.

Uranium is not expected to be a major limitation in this flowsheet, since CHALMEX corresponds to a GANEX Cycle II-type step where uranium should remain at trace levels following high recovery in Cycle I. In contrast, neptunium represents a more critical challenge, and improved control of its oxidation state is likely to enhance its behavior by favoring more stable complexation and more predictable distribution during the process.

In the stripping section using glycolic acid, high recovery of the studied actinides was achieved, corresponding to approximately 98% recovery in a single contactor stage. Partial lanthanide stripping was observed (typically 5–15%, particularly for heavier lanthanides), which corresponds to about 2.5% relative to the feed under the conditions examined. In addition, less than 1% of the loaded organic inventory of Ni, Cu, Fe, and Cd transferred to the strip solution. For metals controlled by masking agents (e.g., Zr, Mo, and Pd), the concentrations measured in the strip liquor were very low (below 0.001%), indicating effective suppression of their transfer under the applied conditions.

6. Summary:

Used nuclear fuel contains long-lived actinides that dominate the long-term radiotoxicity of nuclear waste. Recycling strategies can reduce the required repository timescale but rely on robust liquid–liquid solvent extraction systems that must tolerate high acidity and intense radiation fields. A key challenge is radiolytic degradation of the organic phase, which can change phase behavior, slow kinetics, and reduce extraction performance.

Slope analysis indicated a solvating extraction mechanism for DBOA, consistent with formation of neutral nitrato adducts, $UO_2(NO_3)_2 \cdot 2DBOA$ for U(VI), whereas extraction of trivalent metals was governed primarily by $CyMe_4$-BTBP. Under γ-irradiation up to 300 kGy, extraction of U, Pu, Am, and Cm remained relatively stable in simplified actinide-only solutions, while Np extraction decreased with dose, consistent with radiation-driven redox changes. In simulated raffinate, extraction decreased more strongly indicating important matrix effects and altered kinetics/phase properties. Increased contact time partially restored extraction, supporting a kinetics limitation rather than complete loss of extractant functionality. FS-13 showed high radiolytic stability; neat DBOA displayed FTIR changes, but dilution in FS-13 improved overall stability. UV–Vis features consistent with $HONO/NO_2$ species suggest that nitric-acid radiolysis products can influence extraction kinetics, highlighting solvent washing as a practical mitigation step.

Batch flowsheet tests identified nitrate activity as critical during scrubbing: low-nitrate scrubs caused significant U and Np losses, while nitrate-enriched scrubs improved actinide retention in both solvents. Lanthanide removal was only weakly dependent on scrub composition, typically removing ~40–50% of light lanthanides and ~20–25% of heavier lanthanides per scrub stage.

For stripping, 0.5 M glycolic acid (pH ≈ 4) was the most robust reagent, providing near-quantitative back-extraction of U, Pu, Am, and Np from both solvents (typically ~97–99% for DBOA in a single contact).in addition minor co-stripping of fission products was observed, as example, around 2.5% Sm from the feed remained as an impurity in the stripped product after a single-contact experiment. Dilute nitric-acid stripping was more sensitive to acid carryover and less uniformly effective in single-stage tests, although it remains attractive from an integration perspective because it produces a nitrate product stream compatible with sol–gel routes.

7. Conclusion:

This work evaluates a monoamide-based CHALMEX solvent where tributyl TBP is fundamentally replaced by DBOA, while keeping the benchmark nitrogen-donor ligand $CyMe_4$-BTBP in the same process diluent (FS-13).

Overall, DBOA–$CyMe_4$-BTBP/FS-13 performed comparably to the TBP–$CyMe_4$-BTBP system for actinide extraction and actinide/lanthanide separation, under the investigated conditions, demonstrating that TBP can be substituted by DBOA without compromising the key separation functions of the CHALMEX concept. There was even one advantage. The higher Pu extraction observed for the DBOA-based solvent further indicates potential advantages for Pu-rich feeds streams such as expected in a Gen IV system.

In addition, the monoamide-based solvent showed improved stability under irradiation, as its degradation products were mainly non-phosphorus species (e.g., smaller amides, amines, and carboxylic acids) that did not significantly compromise extraction performance or phase behavior under the investigated conditions and are generally less persistent and less strongly metal-complexing than acidic phosphate species, thereby easing solvent management.

8. Future Work:

Future work can be in different paths, focus on advancing the CHALMEX solvent system toward more process-relevant conditions, particularly counter-current operation, and on strengthening the mechanistic understanding needed for scale-up and integration with downstream recycling.

Future work will focus on quantifying stagewise neptunium redox speciation throughout the flowsheet to determine how acidity, redox environment, and phase composition control the Np oxidation-state distribution and its extraction behavior. The resulting understanding will be used to optimize process conditions and define operating windows that improve neptunium control and separation performance.

The kinetics mechanisms governing extraction and stripping will be studied to better understand mass-transfer limitations, rate-controlling steps, and the influence of hydrodynamics, providing data needed for contactor design and counter-current modelling.

Metal loading, especially with Plutonium, should be investigated to evaluate the behavior of monoamide extraction under more realistic conditions, including potential impacts on distribution ratios, third-phase formation risk, and solvent performance.

A dedicated solvent clean-up stage will be developed to remove fission/corrosion products and radiolysis degradation products after irradiation, supporting solvent lifetime and stable operation.

Progress toward a fully CHON principle implementation will be pursued by replacing the current diluent with a CHON-compatible polar diluent while maintaining acceptable physical properties and separation performance.

To move from batch assessment to continuous-operation evaluation, the solvent system should be evaluated under continuous-operation conditions relevant for deployment. Counter-current extraction and operation in a centrifugal contactor should be used to assess phase behavior, mass-transfer performance, and process stability under realistic hydrodynamic conditions. These results will confirm whether DBOA can be considered a practical extractant within the CHALMEX method and will provide the basis for evaluating scale-up.

Process development should be aligned with downstream recycling and fabrication needs at Chalmers University of Technology by defining product specifications and interface requirements early and ensuring the flowsheet delivers an output stream compatible with the intended fabrication routes.

9. Acknowledgments

This work was carried out within the framework of the ANItA collaboration (Academic-industrial Nuclear Technology Initiative to Achieve a Sustainable Energy Future). Financial support from the Swedish Energy Agency is gratefully acknowledged (project number 52680-1).

Many people have helped and inspired me during my time in this department. First, I would like to thank my supervisors. Christian Ekberg, thank you for giving me the opportunity, for the valuable discussions, and for your guidance in all kinds of situations. My co-supervisor, Marcus Hedberg, thank you for your generous help and encouragement throughout this journey. Your help with daily tasks, and your constant support, have been truly invaluable to me.

I would also like to thank my examiner, Teodora Retegan Vollmer, for welcoming me into the group from day one and for her kind support and help. My sincere thanks to Mark Foreman for the many interesting discussions, not only about science, and for his excellent scientific advice. Thank you to Stefan and Stellan for always being helpful, for listening, and for answering my questions.

I would like to thank everyone at Nuclear Chemistry and Industrial Materials Recycling. You have all contributed to making this department a friendly and enjoyable place to work, and I truly appreciate your support and encouragement. Special thanks to my office mates, Mariam, Letizia, and Deise, for the warmth, kindness, and great company.

Finally, I would like to thank my sweet family, my parents and my siblings, for their unwavering love, care, and support. A special heartfelt thanks to my husband, Eyad, for his love and encouragement, and for being my safe place. And to my beloved children, Basma and Hozaifa: thank you for the joy and light you bring to my life, for the strength you give me to continue, and for filling my heart with love every single day.

10. Reference

1. Çam, E., Casanovas, M. & Moloney, J. *Electricity 2025 - Analysis and Forecast to 2027*. *INTERNATIONAL ENERGY AGENCY* https://www.iea.org/reports/electricity-2025 (2025).
2. Bulle, I. & Tin, B. E. BULL E TIN NET ZERO. *IAEA's Flagsh. Publ.* 66 (2024).
3. World Nuclear Association. World Nuclear Performance Report 2025 - World Nuclear Association. *World Nucl. Assoc.* (2025).
4. Berglöf, C. *Interim Report: The Nuclear New-Build Coordinator's Recommendations Regarding the Expansion of New Nuclear Power in Sweden – June 2024*. https://www.regeringen.se/regeringens-politik/energi/fragor-och-svar-om-karnkraft/ (2024).
5. IAEA-TRS 240. Guidebook on spent fuel storage options and systems. *Guideb. Spent Fuel Storage Options Syst.* 1–178 (2024).
6. Development, N. Advanced Nuclear Fuel Cycles and Radioactive Waste Management.
7. Beatty, R. *Assessment of Nuclear Energy Systems Based on a Closed Nuclear Fuel Cycle with Fast Reactors*. (2012).
8. Nuclear Energy Agency (NEA), O. for E. C. and D. (OECD). *Unlocking the Hidden Value of Nuclear Fuel: The Societal Benefits of Diverse Material Recycling*. (2024).
9. (NEA), N. E. A. *Summary Report of the 16th Information Exchange Meeting on Actinide and Fission Product Partitioning and Transmutation (16IEMPT)*. vol. 13 (2023).
10. NEA. *Strategies and Considerations for the Back End of the Fuel Cycle*. *Nuclear Technology Development and Economics Strategies* (2021).
11. Energy, S. C. International conference on fast reactors and related fuel cycles - challenges and opportunities- (FR 09). *Atomos* **52**, 46 (2010).
12. Lyseid Authen, T. *et al.* Batch flowsheet test for a GANEX-type process: the CHALMEX FS-13 process. *Solvent Extr. Ion Exch.* **40**, 189–202 (2022).
13. Halleröd, J., Ekberg, C., Löfström-Engdahl, E. & Aneheim, E. Development of the chalmers grouped actinide extraction process. *Nukleonika* **60**, 829–835 (2015).
14. Halleröd, J. *et al.* On the Basic Extraction Properties of a Phenyl Trifluoromethyl Sulfone-Based GANEX System Containing CyMe4-BTBP and TBP. *Solvent Extr. Ion Exch.* **36**, 360–372 (2018).
15. Aneheim, E., Ekberg, C., Modolo, G. & Wilden, A. Single Centrifugal Contactor Test of a Proposed Group Actinide Extraction Process for Partitioning and Transmutation Purposes. *Sep. Sci. Technol.* **50**, 1554–1559 (2015).
16. Burger, L. L. *THE CHEMISTRY OF TRIBUTYL PHOSPHATE A REVIEW*. (1958).
17. Lan, T., Liu, J. & Liu, Y. Research on the degradation mechanism, product effects and optimization strategy of the tributyl phosphate solvent system in the PUREX process. *Smart Mol.* (2026) doi:10.1002/smo2.70034.

18. Delegard, Calvin H.; Casella, A. J. Literature Review: Crud Formation at the Liquid/Liquid Interface of TBP-Based Solvent-Extraction Processes. *Pacific Northwest Natl. Lab.* 119–126 (2018) doi:10.5771/9783845298832-119.

19. Lloyd, M. & Fellows, R. Alpha radiolysis and other factors affecting hydrolysis of tributyl phosphate. (1985).

20. Energy, U. S. D. of. *Nuclear Physic and Reactor Theory 1*. vol. 1 (1993).

21. Gregory Choppin, Jan-Olov Liljenzin, Jan Rydberg, C. E. *Radiochemistry and Nuclear Chemistry*. (Academic Press, 2014).

22. IAEA. *Practices for Interim Storage of Research Reactor Spent Nuclear Fuel*. www.iaea.org/publications (2022).

23. Dangouleme, D. *et al.* IAEA review on fuel failures in water cooled reactors. *LWR Fuel Perform. Meet. Fuel/WRFPM 2010* 199–209 (2010).

24. Citation, S. *Safety and Security of Commercial Spent Nuclear Fuel Storage : Public Report COMMERCIAL SPENT NUCLEAR*. (2006). doi:10.17226/11263.

25. NEA & OECD. *Nuclear Science Minor Actinide Burning in Thermal Reactors Systems*. www.oecd.org/publishing/corrigenda. (2013).

26. Feiveson, H., Mian, Z., Ramana, M. V. & von Hippel, F. Spent Fuel from Nuclear Power Reactors: An Overview of a New Study by the International Panel on Fissile Materials. *Int. Panel Fissile Mater.* 1–21 (2011).

27. Rossiello, L. A. & Failla, L. *Classification of Radioactive Wastes, A Safety Guide*. *IAEA* vol. 55 (1994).

28. Andra – ASN - CEA - IRSN. *Radioactive Waste Management Programmes in OECD/NEA Member Countries: France*. (2014).

29. Svensk Kärnbränslehantering AB. R-10-40 Utvecklingen av KBS-3-metoden: Genomgång av forskningsprogram, säkerhets- analyser, myndighetsgranskningar samt SKB:s internationella forskningssamarbete. 272 (2010).

30. SKB. Long-term safety for KBS-3 repositories at Forsmark and Laxemar – a first evaluation : Main Report of the SR-Can project. *Tech. Rep.* **TR-06-09**, 613 (2006).

31. Madic, C. & Hudson, M. *High-Level Liquid Waste Partitioning by Means of Completely Incinerable Extractants*. (1998).

32. Alain Leudet; Bernard Boullis; Charles Madic. Minor Actinide Separation: Recent Advances at the CEA. in *Actinide and Fission Product Partitioning and Transmutation: Proceedings of the Fourth International Information Exchange Meeting* (1997).

33. Strålsäkerhetsmyndigheten (SSM). *Översyn Av Beredskapszoner Bilaga 5-Centralt Mellanlager För Använt Kärnbränsle*. www.stralsakerhetsmyndigheten.se (2017).

34. (SKB), Swedish N. F. and W. M. C. *Deep Repository for Spent Nuclear Fuel: SR 97 – Post-Closure Safety*.

35. AB, S. K. *Program För Forskning, Utveckling Och Demonstration Av Metoder För Hantering Och Slutförvaring Av Kärnavfall Och Använt Kärnbränsle*.

36. Hedin, A. SKB Technical Report 97–13, Swedish Nuclear Fuel and Waste Management Co., Stockholm. (1997).

37. NEA. *Homogeneous versus Heterogeneous Recycling of Transuranics in Fast Nuclear Reactors*. (2012).

38. Salvatores, M. & Palmiotti, G. Radioactive waste partitioning and transmutation within advanced fuel cycles: Achievements and challenges. *Prog. Part. Nucl. Phys.* **66**, 144–166 (2011).

39. Irish, E. R. & Reas, W. H. The PUREX process-a solvent extraction reprocessing method for irradiated uranium. *United States At. Energy Comm. [Unclassified Declassif. Reports Publ. by At. Energy Comm. Its Contract.* **TID-7534**, 83–106 (1957).

40. Idaho National Laboratory. *Nuclear Fuel Reprocessing*. (2010).

41. Gerber, M. S. *A Brief History of the PUREX and UO3 Facilities*. https://www.osti.gov/biblio/10115226%0Ahttps://www.osti.gov/servlets/purl/10115226 (1993) doi:10.2172/10115226.

42. Baron, P. *et al.* Separation of the minor actinides : the DIAMEX-SANEX concept To cite this version : HAL Id : cea-03541464. (2022).

43. Authen, T. L. *et al.* An overview of solvent extraction processes developed in Europe for advanced nuclear fuel recycling , Part 2 — homogeneous recycling. *Sep. Sci. Technol.* **57**, 1724–1744 (2022).

44. Beauvy, M. *et al. Treatment and Recycling Actinide Partitioning – Application to Waste Management Contributors to Articles in This Monograph :*

45. Carrott, M. *et al.* Development of a new flowsheet for co-separating the transuranic actinides : The " EURO-GANEX " process To cite this version : HAL Id : cea-03541573. (2022).

46. Verlinden, B. *et al.* Solvent Optimization Studies for a New EURO- GANEX Process with 2 , 2 ' -Oxybis (N , N -di- n - decylpropanamide) (mTDDGA) and Its Radiolysis Products Solvent Optimization Studies for a New EURO-GANEX. *Solvent Extr. Ion Exch.* **41**, 59–87 (2023).

47. Gregory Choppin, Jan-Olov Liljenzin, Jan Rydberg, and C. E. *Radiochemistry and Nuclear Chemistry*. (Academic Press, 2013). doi:https://doi.org/10.1016/C2011-0-07260-5.

48. Kruse, S. J., Scherrer, S. K., Laverne, J. A., Forbes, T. Z. & Horne, G. P. INORGANIC CHEMISTRY FRONTIERS The inorganic chemist ' s guide to actinide radiation chemistry : a review †. 6398–6434 (2025) doi:10.1039/d5qi00975h.

49. *The Chemistry of the Actinide and Transactinide Elements*. (Springer, 2006).

50. G. Adamson, M. Chemical thermodynamics of uranium. *J. Nucl. Mater.* **200**, 154–155 (1993).

51. Lemire, R. J. *et al. NEA, Chemical Thermodynamics of Neptunium and Plutonium*. *Chemical Thermodynamics* vol. C (2001).

52. Choppin, G. R. Actinide speciation in aquatic systems. in *Marine Chemistry* vol. 99 83–92 (2006).

53. Bilewicz, A. Ionic radii of heavy actinide(III) cations. *Radiochim. Acta* **92**, 69–72 (2004).

54. Greenwood, N. N.; Earnshaw, A. *Chemistry of the Elements*. (Butterworth-Heinemann, 1997).

55. Zhu, Q., Zhu, J. & Zhu, C. Recent progress in the chemistry of lanthanide-ligand multiple bonds. *Tetrahedron Lett.* **59**, 514–520 (2018).

56. Kaufholz, P. *The Selective Separation of Am(III) from Highly Radioactive PUREX Raffinate*. *Energie & Umwelt* vol. 402 (2017).

57. Union, I., Pure, O. F. & Chemistry, A. INTERNATIONAL UNION OF PURE NOMENCLATURE FOR LIQUID-LIQUID DISTRIBUTION (SOLVENT EXTRACTION) Nomenclature for liquid-liquid distribution (solvent extraction) (IUPAC Recommendations 1993) Introduction *Pure Appl. Chem.* **65**, 2373–2396 (1993).

58. Rydberg, J., Cox, M., Musikas, C. & Choppin, G. R. *Solvent Extraction and Practice*. (2004).

59. Vladimir S Kislik. *Solvent Extraction Classical and Novel Approaches*. (Elsevier B.V., 2011).

60. Danesi, P. R., Chiarizia, R. & Coleman, C. F. The kinetics of metal solvent extraction. *C R C Crit. Rev. Anal. Chem.* **10**, 1–126 (1980).

61. El-Hefny, N. E. Chemical kinetics and reaction mechanisms in solvent extraction: New Trends and applications. *J. Phys. Sci.* **28**, 129–156 (2017).

62. Yeremin, E. N. The foundations of chemical kinetics. *J. Franklin Inst.* **269**, 248 (1960).

63. Stevens, G. W., Lo, T. C. & Baird, M. H. I. *Extraction, Liquid–Liquid*. *Kirk-Othmer Encyclopedia of Chemical Technology* (2018). doi:10.1002/0471238961.120917211215.a01.pub3.

64. Kato, S. & Kansha, Y. *Comprehensive Review of Industrial Wastewater Treatment Techniques*. *Environmental Science and Pollution Research* vol. 31 (Springer Berlin Heidelberg, 2024).

65. Réaux-Durain, J. *et al.* Back-extraction of major actinides from organic phase through precipitation. *Comptes Rendus Chim.* **27**, 143–152 (2024).

66. Lyseid Authen, T. *et al.* Batch Tests for Optimisation of Solvent Composition and Process Flexibility of the CHALMEX FS-13 Process. *Solvent Extr. Ion Exch.* **39**, 1–17 (2021).

67. Babain, V., Alyapyshev, M., Ekberg, C. & Todd, T. Fluorinated Diluents- A Review. *Solvent Extr. Ion Exch.* **41**, 253–291 (2023).

68. Halleröd, J., Ekberg, C. & Aneheim, E. Phenyl trifluoromethyl sulfone as diluent in a grouped actinide extraction process: extraction properties of the solvent components TBP and CyMe4-BTBP. *J. Radioanal. Nucl. Chem.* **307**, 1711–1715 (2016).

69. Manchanda, V. K. & Pathak, P. N. *Amides and Diamides as Promising Extractants in the Back End of the Nuclear Fuel Cycle: An Overview*. *Separation and Purification Technology* vol. 35 (2004).

70. Ravi, J., Mishra, S., Pandey, N. K., Mallika, C. & Kamachi Mudali, U. *Feasibility Studies of Using N,N-Dihexyloctanamide (DHOA) for Fast Reactor Fuel Reprocessing Applications*. *Radiochimica Acta* vol. 106 (2018).

71. McCann, K., Mincher, B. J., Schmitt, N. C. & Braley, J. C. *Hexavalent Actinide Extraction Using N,N-Dialkyl Amides*. *Industrial and Engineering Chemistry Research* vol. 56 (2017).

72. Pathak, P. N., Kumbhare, L. B. & Manchanda, V. K. *Structural Effects in n N-Dialkyl Amides on Their Extraction Behavior toward Uranium and Thorium*. *Solvent Extraction and Ion Exchange* vol. 19 (2001).

73. Stoughton, R. W. Effects of Structure of , -Disubstituted Amides on Their. **IX**, 66–69 (1960).

74. Condamines, N. & Musikas, C. The extraction by N,N-dialkylamides. I, HNO, and other inorganic acids. *Solvent Extr. Ion Exch.* **6**, 1007–1034 (1988).

75. Jay-Gerin, J. P. Fundamentals of Water Radiolysis. *Encyclopedia* **5**, 1–19 (2025).

76. Mincher, B. J. *et al.* Review Article : The Effects of Radiation Chemistry on Solvent Extraction : 1 . Conditions in Acidic Solution and a Review of TBP Radiolysis Review Article : The Effects of Radiation Chemistry. **6299**, (2009).

77. Horne, G. P. *et al.* Effect of Chemical Environment on the Radiation Chemistry of N , N-di- (2- ethylhexyl) butyramide (DEHBA) and Plutonium Retention. (2019).

78. Katsumura, Y. *et al.* Pulse radiolysis study of aqueous nitric acid solutions. Formation mechanism, yield, and reactivity of NO3 radical. *J. Phys. Chem.* **95**, 4435–4439 (1991).

79. Sugai, H. Crud in solvent washing process for nuclear fuel reprocessing. *J. Nucl. Sci. Technol.* **29**, 445–453 (1992).

80. Authen, T. L. Advances in the application and understanding of the CHALMEX FS-13 Process. (CHALMERS UNIVERSITY OF TECHNOLOGY, 2022).

81. Ekberg C., Löfström-Engdahl E., Aneheim E., Foreman M., Geist A., Lundberg D., Denecke M., Perssonc I. The structures of CyMe4-BTBP complexes of americium(III) and europium(III) in solvents used in solvent extraction, explaining their separation properties. **32**, 167–186 (2021).

82. Gogolski, J. M., Zalupski, P. R., Grimes, T. S. & Jensen, M. P. *Neptunium Extraction by N,N-Dialkylamides*. *Radiochimica Acta* vol. 108 (2020).

83. Edwards, A. C. *et al.* Exploring electronic effects on the partitioning of actinides(III) from lanthanides(III) using functionalised bis-triazinyl phenanthroline ligands. *Dalt. Trans.* **45**, 18102–18112 (2016).

84. Aneheim, E., Ekberg, C., Foreman, M. R. S., Löfström-Engdahl, E. & Mabile, N. Studies of a solvent for GANEX applications containing CyMe 4-BTBP and DEHBA in cyclohexanone. *Sep. Sci. Technol.* **47**, 663–669 (2012).

85. Halleröd, J., Ekberg, C., Löfström-Engdahl, E. & Aneheim, E. *Development of the Chalmers Grouped Actinide Extraction Process*. *Nukleonika* vol. 60 (2015).

86. Mincher, B. J. *et al.* The redox chemistry of neptunium in γ-irradiated aqueous nitric acid. *Radiochim. Acta* **101**, 259–265 (2013).

87. Distler, P. *et al.* Stability of Different BTBP and BTPhen Extracting or Masking Compounds against γradiation. *ACS Omega* **6**, 26416–26427 (2021).

88. Verma, P. K., Gujar, R. B., Kanekar, A. S., Bhardwaj, Y. K. & Mohapatra, P. K. E ff ect of irradiation on the hydrodynamic parameters and extraction e ffi ciency of several frequently used ionic liquids. *Radiat. Phys. Chem.* **158**, 180–187 (2019).

89. Belova, E. V, Skvortsov, I. V, Kadyko, M. I. & Yudintsev, S. V. The effect of irradiation on hydrodynamic properties of extraction mixtures based on diamides of N-heterocyclic dicarboxylic acids in heavy fluorinated diluents. **51**, 1163–1168 (2019).

Appendixes

Appendix 1:

Table 4. Composition of inorganic elements used in the simulated raffinate solution

Elements	**Salts**	Concentration **mg.L^{-1}**	Concentration **mM**
Ag	$AgNO_3$	6.88	0.06
Al	$Al(NO_3)_3.9H_2O$	4.7	0.17
Ba	$Ba(NO_3)_2$	225	1.64
Cd	$Cd(NO_3)_2.4H_2O$	14.1	0.13
Ce	$(NH_4)_2[Ce(NO_3)_6]$	473.3	3.38
Cr	$Cr(NO_3)_3.9H_2O$	76.7	1.48
Cs	$CsNO_3$	452.8	3.41
Cu	$Cu(NO_3)_2.3H_2O$	16.5	0.26
Eu	$Eu(NO_3)_3.5H_2O$	28.1	0.18
Fe	$Fe(NO_3)_3.9H_2O$	1545	27.67
Gd	$Gd(NO_3)_3.6H_2O$	21.1	0.13
La	$La(NO_3)_3.6H_2O$	197.3	1.42
Mo	MoO_3	548	5.71
Na	$NaNO_3$	1237.5	53.83
Nd	$Nd(NO_3)_3.6H_2O$	92.2	0.64
Ni	$Ni(NO_3)_2.6H_2O$	38.4	0.65
Pd	$Pd(NO_3)_2.2H_2O$	86.9	0.82
Pr	$Pr(NO_3)_3.6H_2O$	184.8	1.31
Ru	$RuCl_3.H_2O$	320.3	3.17
Rb	$RbNO_3$	54.4	0.64
Sb	Sb_2O_3	3.3	0.03
Se	SeO_2	9.7	0.09
Sm	$Sm(NO_3)_3.6H_2O$	122.1	0.83
Sn	$SnCl_2.2H_2O$	9.8	0.00
Sr	$SrCO_3$	142.4	2.33
Te	TeO_2	88.7	0.70
Y	$Y(NO_3)_3$	74.6	0.84
Zr	$ZrO(NO_3)_2.H_2O$	676.1	10.09

Appendix 2:

Table 5. Radionuclide Activities/concentration in the Stock Solution

Isotope	**Activities /Concentration**
Pu-239	0.6 MBq/mL
Am-241	2.2 MBq/mL
Np-237	0.030 MBq/mL
Cm-244	0.074 MBq/mL
Eu-152	4 MBq/ mL
Uranium (nat)	0.017 mol/L

Appendix 3: Table 6. Molecular structure

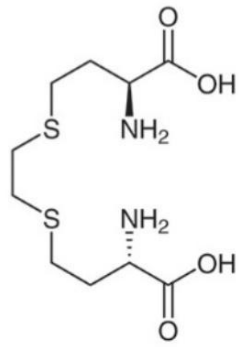	Bimet
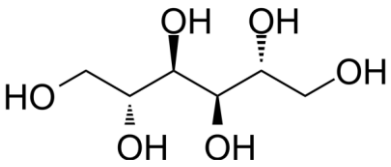	D-mannitol
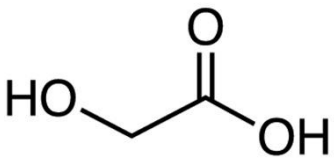	Glycolic acid